

See discussions, stats, and author profiles for this publication at: <https://www.researchgate.net/publication/354740183>

# Body Size Disparity of the Archosauromorph Reptiles during the First 90 Million Years of Their Evolution

Article in AMEGHINIANA · January 2022

DOI: 10.5710/AMGH.16.09.2021.3441

---

CITATIONS

9

READS

276

3 authors:



[Luciano Agustín Pradelli](#)

Museo Argentino de Ciencias Naturales "Bernardino Rivadavia"

2 PUBLICATIONS 25 CITATIONS

[SEE PROFILE](#)



[Juan Martín Leardi](#)

National Scientific and Technical Research Council

36 PUBLICATIONS 637 CITATIONS

[SEE PROFILE](#)



[Martin Ezcurra](#)

Museo Argentino de Ciencias Naturales "Bernardino Rivadavia"

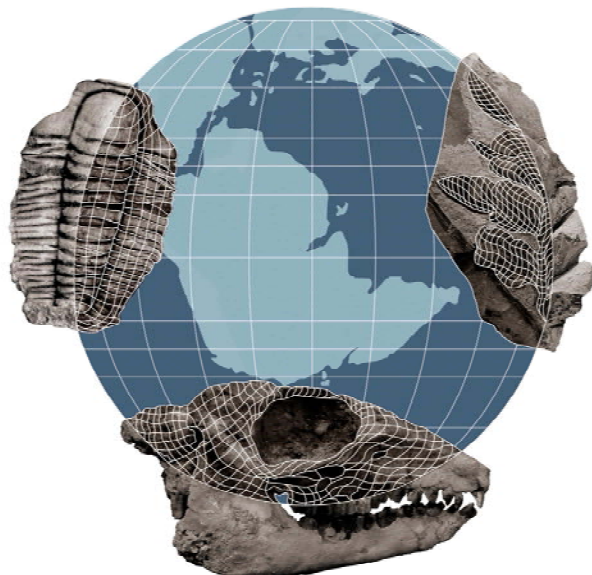
202 PUBLICATIONS 5,289 CITATIONS

[SEE PROFILE](#)



# AMEGHINIANA

A GONDWANAN PALEONTOLOGICAL JOURNAL



This file is an uncorrected accepted manuscript (i.e., postprint). Please be aware that during the production process this version will definitely change. This postprint will be removed once the paper is officially published.

All legal disclaimers that apply to the journal pertain.

---

**Submitted:** April 5<sup>th</sup>, 2021 – **Accepted:** September 16<sup>th</sup>, 2021 – **Posted online:** September 28<sup>th</sup>, 2021

To link and cite this article:

**doi:** [10.5710/AMGH.16.09.2021.3441](https://doi.org/10.5710/AMGH.16.09.2021.3441)

PLEASE SCROLL DOWN FOR ARTICLE

---

1   **BODY SIZE DISPARITY OF THE ARCHOSAUROMORPH REPTILES**  
2   **DURING THE FIRST 90 MILLION YEARS OF THEIR EVOLUTION**  
3   DISPARIDAD DEL TAMAÑO CORPORAL DE LOS REPTILES  
4   ARCOSAUROMORFOS DURANTE LOS PRIMEROS 90 MILLONES DE AÑOS DE  
5   SU EVOLUCIÓN

6  
7   LUCIANO A. PRADELLI<sup>1,2</sup>, JUAN M. LEARDI<sup>2,3,4</sup>, AND MARTÍN D. EZCURRA<sup>1,2</sup>  
8

9   <sup>1</sup>Sección Paleontología de Vertebrados CONICET–Museo Argentino de Ciencias  
10   Naturales “Bernardino Rivadavia”, Avenida Ángel Gallardo 470, C1405DJR, Buenos  
11   Aires, Argentina. *lucianopradielli@gmail.com, martindezcurra@yahoo.com.ar*

12   <sup>2</sup>Consejo Nacional de Investigaciones Científicas y Técnicas (CONICET), Godoy Cruz  
13   2290, C1425FQB, Buenos Aires, Argentina.

14   <sup>3</sup>Instituto de Estudios Andinos “Don Pablo Groeber” (IDEAN, UBA-CONICET),  
15   Departamento de Ciencias Geológicas, Facultad de Ciencias Exactas y Naturales,  
16   Universidad de Buenos Aires, Intendente Güiraldes 2160, C1428EGA, Buenos Aires,  
17   Argentina. *jmleardi@gl.fcen.uba.ar*

18   <sup>4</sup>Departamento de Biodiversidad y Biología Experimental, Facultad de Ciencias Exactas  
19   y Naturales, Universidad de Buenos Aires, Intendente Güiraldes 2160, C1428EGA,  
20   Buenos Aires, Argentina.

21  
22   58 pages (text+references), 13 Figures, 3 Supplementary Online Information  
23

24   Proposed header: PRADELLI *ET AL.*: ARCHOSAUROMORPH BODY SIZE  
25   DISPARITY

26

27 Short description: Body size disparity and body size variation through palaeolatitudinal  
28 distribution of archosauromorphs during their early evolutionary radiation.

29

30

31

32

33

34

35

36

37

38

39

40

41

42

43

44

45

46

47

48

49

50

51    **Abstract**

52    An important parameter in the study of the macroevolutionary history of a clade is the  
53    variation of its body size. However, the study of this parameter in archosauromorphs  
54    has been restricted to Archosauria and the disparity in body size has not been  
55    exhaustively explored. In the present work we explore the variation in body size of  
56    more than 400 known Permian–Early Jurassic archosauromorph species in the context  
57    of their early evolutionary radiation. We analysed the disparity of body size over time  
58    and the relationship between this parameter and the palaeolatitudinal distribution of  
59    species. From these analyses, it was found that the disparity of body size of  
60    archosauromorphs increased after the Permian/Triassic boundary. In the case of  
61    Pseudosuchia and Pan-Aves (=Avemetatarsalia), the Triassic-Jurassic extinction seems  
62    to show a pattern of selective extinction of medium to large-sized forms and their body  
63    size disparity decreased significantly. In contrast, dinosaurs increased in body size and  
64    disparity did not change significantly after the Triassic/Jurassic extinction event.  
65    Regarding the relationship between body size and geographic distribution,  
66    pseudosuchians show a pattern of decrease of body size towards higher palaeolatitudes,  
67    *i.e.*, a converse Bergman's Rule. These results could be linked to physiological factors  
68    since many groups of extant heterothermic animals show a similar pattern. These  
69    analyses help elucidating the complex body size evolutionary dynamics in the early  
70    radiation of Archosauromorpha, as indicated by the different patterns observed across  
71    its subclades.

72    **Key Words**

73    Archosauromorpha. Diapsida. Macroevolution. Evolutionary radiation. Palaeolatitude.  
74    Bergmann's Rule.

75

76 **Resumen**

77 Un parámetro importante en el estudio de la historia macroevolutiva de un clado es la  
78 variación de su tamaño corporal. Sin embargo, el estudio de este parámetro en  
79 arcosauroomorfos ha estado restringido a Archosauria y la disparidad del tamaño  
80 corporal no se ha explorado exhaustivamente. En el presente trabajo exploramos la  
81 variación del tamaño corporal de más de 400 especies conocidas de arcosauroomorfos del  
82 Pérmico–Jurásico Temprano en el contexto de su radiación evolutiva temprana.  
83 Analizamos la disparidad del tamaño corporal a lo largo del tiempo y la relación entre  
84 este parámetro y la distribución paleolatitudinal de las especies. A partir de estos  
85 análisis, se encontró que la disparidad del tamaño corporal de los arcosauroomorfos  
86 aumentó después del límite Pérmico/Triásico. En el caso de Pseudosuchia y Pan-Aves  
87 (=Avemetatarsalia), la extinción triásica/jurásica parece mostrar un patrón de extinción  
88 selectiva de formas de tamaño mediano a grande y su disparidad de tamaño corporal  
89 disminuyó significativamente. En contraste, los dinosaurios aumentaron su tamaño  
90 corporal y su disparidad no cambió significativamente después del evento de extinción  
91 del límite Triásico/Jurásico. En cuanto a las relaciones entre el tamaño corporal y la  
92 distribución geográfica, los pseudosuquios muestran un patrón de disminución del  
93 tamaño corporal hacia paleolatitudes más altas, *i.e.*, Regla de Bergmann inversa. Estos  
94 resultados pueden deberse a factores fisiológicos ya que muchos grupos de animales  
95 heterotermos actuales muestran este patrón. Estos análisis ayudan a dilucidar las  
96 complejas dinámicas evolutivas del tamaño corporal en la evolución temprana del  
97 grupo, como lo indican los diferentes patrones observados a lo largo de sus subclados.

98 **Palabras clave**

99 Archosauroomorpha. Diapsida. Macroevolución. Radiación evolutiva. Paleolatitud.  
100 Regla de Bergmann.

101 ARCHOSAUROMORPHA includes all diapsids more closely related to dinosaurs  
102 (including birds) and crocodilians than to lepidosauromorphs (Gauthier *et al.*, 1988).  
103 The oldest records of the group correspond to body fossils from middle–upper Permian  
104 rocks of Europe and possibly South America (Ezcurra *et al.*, 2014, 2015; Martinelli *et*  
105 *al.*, 2017) and ichnofossils from the upper Permian of Europe (Bernardi *et al.*, 2015).  
106 These Permian archosauromorph records are scarce, but the group subsequently  
107 diversified in the Triassic to numerically dominate Mesozoic continental ecosystems  
108 (Benton, 1983) and include the evolutionary radiation of birds during the Cenozoic  
109 (Feduccia, 1995). As a consequence, the study of the early archosauromorph evolution  
110 is crucial in understanding the establishment of the post-Triassic terrestrial ecosystems  
111 and the modern taxonomic richness of the group, which includes more than 10,000  
112 extant avian species (Clements, 2007).

113 The early evolutionary history of Archosauromorpha during the Triassic is  
114 generally considered one of the most important evolutionary radiations of tetrapods  
115 documented in the fossil record (Bakker, 1977; Benton, 1983). Our knowledge of the  
116 remarkable diversification of early archosauromorphs has considerably increased in the  
117 last ten years thanks to intensive research efforts, which resulted, for example, in the  
118 description of approximately 60 new Triassic archosauromorph species (see Nesbitt *et*  
119 *al.*, 2013; Ezcurra & Butler, 2018). These studies have increased not only the taxonomic  
120 diversity of the group and the magnitude of their radiation, but also their morphological  
121 disparity, including the presence of phenotypes convergent to those of some Cretaceous  
122 dinosaur clades (*e.g.*, biped and edentulous poposauroids: Nesbitt & Norell 2006; stem-  
123 archosauriforms with a dome-shaped skull roof: Stocker *et al.*, 2016; Nesbitt *et al.*,  
124 2021; allokotosaurs with a pair of supraorbital horns: Sengupta *et al.*, 2017).  
125 Concurrently, the increase in anatomical information available and improved taxonomic

126 understanding of the group have allowed several new phylogenetic analyses. These  
127 analyses have focused on different lineages and have covered most of the Permo–  
128 Triassic archosauromorph diversity (e.g., Nesbitt, 2011; Dilkes & Arcucci, 2012;  
129 Nesbitt *et al.*, 2015, 2017; Otero *et al.*, 2015; Ezcurra, 2016; Parker, 2016; Sookias,  
130 2016; Ezcurra *et al.*, 2017, 2020a, b, 2021a; Langer *et al.*, 2017; Leardi *et al.*, 2017;  
131 Jones & Butler, 2018; Desojo *et al.*, 2020a).

132 Our knowledge of the timing of early archosauromorph evolution has been  
133 enhanced by several radioisotopic dates of Permo–Triassic archosauromorph-bearing  
134 stratigraphic units all over the world. These analyses have constrained the deposition  
135 ages of these units and allowed us to refine intercontinental and interbasin temporal  
136 correlations (e.g., Irmis *et al.*, 2011; Martínez *et al.*, 2011; Ramezani *et al.*, 2011, 2014;  
137 Liu *et al.*, 2013; Rubidge *et al.*, 2013; Ottone *et al.*, 2014; Marsicano *et al.*, 2016;  
138 Ezcurra *et al.*, 2017; Langer *et al.*, 2018; Wang *et al.*, 2019; Desojo *et al.*, 2020b). This  
139 improved chronostratigraphic framework is crucial in fully understanding the tempo and  
140 mode of macroevolutionary events (Simpson, 1944). This combination of factors and  
141 the recent proliferation of a broad spectrum of quantitative analytical methodologies  
142 have greatly facilitated studies of the macroevolutionary patterns during the adaptive  
143 radiation of Archosauromorpha in the Triassic and Early Jurassic (e.g., Brusatte *et al.*,  
144 2008a, b; Irmis, 2011; Sookias *et al.*, 2012a, b; Turner & Nesbitt, 2013; Ezcurra *et al.*,  
145 2016, 2021b, c; Foth *et al.*, 2016; McPhee *et al.*, 2017; Ezcurra & Butler, 2018).

146 The early evolution of Archosauromorpha took place when all the continents  
147 were merged into a single landmass, Pangaea, and a macroevolutionary scenario  
148 punctuated by the Permian/Triassic (ca. 251 Ma) and Triassic/Jurassic (ca. 200 Ma)  
149 mass extinction events (Raup, 1977; Raup & Sepkoski, 1982; Chen & Benton, 2012).  
150 These mass extinctions have motivated several studies in order to improve our

151 understanding of their impact on different taxonomic groups and the subsequent biotic  
152 recovery (e.g., Looy *et al.*, 1999; Hesselbo *et al.*, 2002; Payne *et al.*, 2004; Grauvogel-  
153 Stamm & Ash, 2005; Whiteside & Ward, 2011; Irmis & Whiteside, 2012; Franceschi *et*  
154 *al.*, 2014). These crises are associated with rapid falls and recoveries of trophic  
155 networks due to ecological redundancy, generating instability and a subsequent  
156 restructuring of ecosystems (Whiteside & Ward, 2011; Irmis & Whiteside, 2012). The  
157 poor archosauromorph record during the Permian hampers a direct evaluation of how  
158 the clade was affected by the Permian/Triassic biotic crisis. However, the presence of  
159 numerous ghost lineages indicates that the origin of many archosauromorph clades  
160 predated this extinction, and that the phylogenetic diversity of the group as a whole was  
161 not substantially affected (Ezcurra & Butler, 2018). After the mass extinction, Ezcurra  
162 and Butler (2018) found that the morphological diversity of archosauromorphs  
163 decreased in the Induan, but increased significantly in the Olenekian. In, the Olenekian  
164 there is major phylogenetic diversification (with the appearance of groups like  
165 rhynchosaurs, erythrosuchids, and crown archosaurs) likely resulting from expansion  
166 into vacant ecological niches. Increase in morphological disparity continued during the  
167 Anisian, but at a lower magnitude, and at the same time the number and abundance of  
168 species increased considerably, which temporally matched the stabilization of  
169 ecosystems as indicated by the end of large perturbations in the carbon cycle (Ezcurra &  
170 Butler, 2018). The Triassic/Jurassic mass extinction produced a second, deep  
171 restructuring of continental ecosystems, but it seems to have affected archosauromorphs  
172 more severely than the Permian/Triassic extinction event. The Triassic/Jurassic event  
173 resulted in the extinction of all archosauromorphs with the exception of those clades  
174 that subsequently dominated the Mesozoic continental ecosystems, namely  
175 crocodylomorphs, pterosaurs and dinosaurs.

176 Among the macroevolutionary studies that focused on the adaptive radiation of  
177 Permo-Triassic archosauromorphs, several authors have analysed the evolution of body  
178 size through time (Sookias *et al.*, 2012a, b; Turner & Nesbitt, 2013; Ezcurra *et al.*,  
179 2016, 2021c; Sengupta *et al.*, 2017). Sookias *et al.* (2012b) found that the evolution of  
180 the early archosauromorph body size was dominated by passive processes (*e.g.*,  
181 Brownian evolution without trend), whereas less inclusive clades showed frequent  
182 events of white noise (stasis). By contrast, Turner and Nesbitt (2013) concluded that the  
183 evolution of the body size of the group was driven by punctuated events, with more  
184 changes during the Early Triassic, and probably a directional trend of body size  
185 increase. In fact, Turner and Nesbitt (2013), Ezcurra *et al.* (2016) and Sengupta *et al.*  
186 (2017) found events of considerable increase in body size of particular Triassic  
187 archosauromorph groups, including allokotosaurs, rhynchososaurs and erythrosuchids.  
188 Similarly, Ezcurra *et al.* (2021c) found an increase in body size disparity and of body  
189 size itself in South American non-archosaurian archosauromorphs towards the Late  
190 Triassic. However, based on Sookias *et al.* (2012b) results, these increases in body size  
191 through time seem to result from passive evolutionary processes rather than from  
192 Cope's Rule *sensu stricto* (multi-lineage active trend towards larger sizes; Cope, 1887),  
193 which appears to be extremely rare in Permian/Jurassic archosauromorphs. This  
194 conclusion agrees with more recent analyses that found that this rule did not apply  
195 during the evolution of rhynchososaurs (Ezcurra *et al.*, 2016) and early crocodylomorphs  
196 (Godoy *et al.*, 2019).

197 Regarding a possible relationship between body size and biogeography, there  
198 has been no study to date investigating this topic in early archosauromorphs. Godoy *et*  
199 *al.* (2019) performed correlation analyses between abiotic factors, such as palaeolatitude  
200 and palaeotemperature, and body size for Triassic to extant crocodylomorphs, but did

not find a correlation during the Triassic–Jurassic time span. By contrast, they found a moderate to strong correlation between body size and palaeotemperature in Crocodylia between the Late Cretaceous and the present. There is evidence for a relationship between body size and palaeolatitudinal variation, where the evolution of body size follows a punctuated model of evolution consistent with periods of environmental change, for crocodylomorphs (Stockdale & Benton, 2021). A recent study on the palaeobiogeographic distribution of Late Triassic tetrapods supported this idea for non-pseudosuchian archosaurs because they had a palaeobiogeographic distribution similar to that of extant endothermic animals (Dunne *et al.*, 2020). By contrast, pseudosuchians were more diverse in warmer environments, as is the case for extant ectothermic reptiles (Dunne *et al.*, 2020). This study also concluded that palaeoclimate could have had a direct influence on the distribution of species during that time span. Palaeoclimate, and hence palaeobiogeography, may have also influenced the body size of early archosauromorphs. For example, the Bergmann’s Rule proposes that populations and species of endothermic animals that inhabit colder environments are larger than those that occur in warmer environments (Bergmann, 1847). On the other hand, the Converse Bergmann’s Rule proposes the inverse effect and has been found for numerous ectothermic species (*e.g.*, insects) (Park, 1949). However, the presence of a correlation between palaeolatitudinal distribution and body size has not been tested so far for Permian to Early Jurassic archosauromorphs. Previous studies have proposed endothermic metabolism for stem-crocodylians based on the heart anatomy of extant species (Seymour *et al.*, 2004). More recently, Cubo and Jalil (2019) expanded this proposal for Triassic archosauromorphs based on palaeohistological evidence.

In the last five years, knowledge of the phylogenetic relationships of early archosauromorphs has expanded considerably, from quantitative analyses that included

226 less than 30 species to datasets that include more than 100 species (*e.g.*, Ezcurra *et al.*,  
227 2020a, b), some of which had never been previously included in a quantitative  
228 phylogenetic analysis (Fig. 1). The volume of phylogenetic information available today,  
229 added to the recent progress in the chronostratigraphy of late Permian–Early Jurassic  
230 continental stratigraphic units, and methodological advances in macroevolutionary  
231 analyses, allows analysis of the body size evolution of early archosauromorphs in a  
232 more comprehensive and exhaustive way than has been done before. The goal of the  
233 current work is to explore the disparity of body size in the first 90 million years of  
234 evolution of Archosauromorpha. In order to do this, we analysed the variation of body  
235 size of archosauromorphs from the Permian to the Early Jurassic in an updated  
236 phylogenetic context and evaluated the impact of mass extinctions on the group's body  
237 size. Furthermore, we analysed the variation of archosauromorph body size in relation  
238 to the palaeolatitudinal distribution of species during this time frame. We aimed to test  
239 the following hypotheses: a) the extinction of the Permian/Triassic boundary did not  
240 produce significant changes in any of the disparity metrics of archosauromorph body  
241 size between the late Permian–Olenekian time span; b) the extinction of the  
242 Triassic/Jurassic boundary produced significant changes in one or more of the disparity  
243 metrics of pseudosuchian archosaur body size between the late Norian–Sinemurian time  
244 span; c) the extinction of the Triassic/Jurassic boundary did not produce significant  
245 changes in none of the disparity metrics of pan-avian (= avemetatarsalian) archosaur  
246 body size between the late Norian–Sinemurian time span; and d) larger  
247 archosauromorphs species have a higher probability to be found in localities located at  
248 higher palaeolatitudes during the Triassic and Early Jurassic, in congruence with  
249 Bergmann's Rule.

250 **MATERIAL AND METHODS**

251    **Construction of the dataset**

252    A list of all currently valid archosauromorph species (plus diagnostic specimens without  
253    a formal assignment to a species-level taxon; species and diagnostic specimens together  
254    are hereafter called ‘species’ for simplicity) recorded between the middle–late Permian  
255    and the Early Jurassic was built, accounting for a total of 403 species. This list was  
256    expanded to a database that included the measurement or estimation of femoral length,  
257    ontogenetic stage, taxonomic group, chronostratigraphic range in millions of years, and  
258    palaeocoordinates taken from first hand observation of specimens, published data, and  
259    the Paleobiology Database specifically in the case of the palaeocoordinates  
260    (<https://paleobiodb.org/>, February 2021).

261           Femoral length was used as an estimator of body size because this element has  
262    been shown to grow isometrically during archosaur ontogeny (Anderson *et al.*, 1985)  
263    and has been widely used in similar studies by previous authors (*e.g.*, Sookias *et al.*,  
264    2012a, b; Turner & Nesbitt 2013; Sengupta *et al.*, 2017). Species body mass was not  
265    calculated because the most robust equations to estimate it are based on the humeral and  
266    femoral shaft circumferences (Anderson *et al.*, 1985; Campione & Evans, 2012, 2020)  
267    and we do not have this measure for most of the sampled species.

268           In the cases in which there was more than one specimen of the same species with  
269    preserved femora, the measurement of the largest specimen was used. In cases where  
270    there was no preserved femur for the known specimens or the largest specimen of the  
271    same species, femoral length was estimated by simple cross-multiplication based on the  
272    length of the skull or other long bone (*e.g.*, humerus, tibia) compared (using a ratio  
273    equation) to the known femoral length of a close relative or a smaller specimen of the  
274    species, respectively (Supplementary Online Information II). Species that did not have  
275    preserved elements that could provide a reliable estimate of femoral length were

276 excluded from the analyses, but were kept in the table for the temporal calibration of the  
277 supertrees (see below). Similarly, those species based on specimens with positive  
278 evidence of a juvenile condition at the time of their death (*e.g.*, based on bone  
279 microstructure anatomy) were also excluded, but not from the temporal calibration of  
280 the supertrees. The final dataset of species with recorded femoral length includes a total  
281 of 323 species. Femoral length measurements were converted to logarithmic scale  
282 ( $\log_{10}$ ) prior to all analyses.

283 **Time bins, taxonomic groups, and disparity measures**

284 Nine time bins were used to analyse the dataset in a temporal framework: 1) middle–late  
285 Permian, 2) Induan, 3) Olenekian, 4) Anisian, 5) Ladinian–early Carnian, 6) late  
286 Carnian–early Norian, 7) middle Norian–Rhaetian, 8) Hettangian–Sinemurian, and 9)  
287 Pliensbachian–Toarcian. This selection of discretised time bins has been used  
288 previously by other authors (Ezcurra, 2010a; Sookias *et al.*, 2012a, b; Button *et al.*,  
289 2017; Ezcurra & Butler, 2018) and aims to: 1) reduce the number of species that occupy  
290 two time bins due to chronostratigraphic uncertainty in their dating, 2) evaluate  
291 evolutionary patterns before and after the mass extinctions, and 3) produce time  
292 intervals of similar duration. In this sense, species (71 species) that occur in more than  
293 one time interval because of their chronostratigraphic uncertainty were excluded from  
294 the analyses because they can hide patterns or generate spurious results. Nevertheless, a  
295 sensitivity analysis was also performed including these species.

296 The dataset was also divided into different taxonomic groups with the object of  
297 evaluating the presence of different patterns across the archosauromorph phylogeny.  
298 The following groups were used for the disparity analysis: 1) non-archosaurian  
299 Archosauromorpha, 2) Pseudosuchia, 3) non-dinosaurian Pan-Aves, 4) Theropoda, 5)  
300 Sauropodomorpha, 6) Ornithischia, and 7) Archosauromorpha (including the entire

dataset; see Supplementary Online Information II). Phytosaurs were considered as pseudosuchians for all these analyses (sensu Ezcurra 2016). In particular, one species (*Guaibasaurus candelariensis*) was included only in group 7 (*i.e.*, with all archosauromorphs) because of its controversial position within Saurischia (*e.g.*, Ezcurra, 2010b; Langer *et al.*, 2011). A caveat is that two of the groups used in our analysis are paraphyletic assemblages: ‘non-archosaurian Archosauromorpha’ and ‘non-dinosaurian Pan-Aves’. The results recovered for these two paraphyletic assemblages should be understood merely as the sum of the trends seen in their different array of lineages and not directly as a trend of the whole group, as these do not represent true evolutionary entities (*i.e.*, monophyletic groups). For example, the recovered patterns of these paraphyletic groups could be the result of the exclusion of their more deeply nested monophyletic groups: Archosauria and Dinosauria, respectively. However, the evaluation of these paraphyletic groups allows a comparison and, hence, better interpretation of the evolutionary patterns found for Archosauria and Dinosauria. Clades within these paraphyletic groups (*e.g.*, Tanystropheidae, Rhynchosauria, Allokotosauria, Proterochampsidae, Pterosauria, Silesauridae) do not have a sample size large enough to explore their evolutionary trends with proper statistical power. Furthermore, paraphyletic groupings have been used previously in other contributions dealing with diversity or macroevolutionary trends in Archosauromorpha (*e.g.*, Godoy *et al.*, 2019; Turner and Nesbitt, 2013), as most analyses (including our own —because we excluded the temporal range—) do not include more deeply nested and younger groups of the clade, such as birds and neosuchians.

The body size diversity of early archosauromorphs was analysed after calculating the mean and the following three disparity metrics based on the femoral length and for each time bin: standard deviation, ranges, and median (Benson, 2018;

326 Guillerme *et al.*, 2020). The standard deviation quantifies the variability and internal  
327 structuring of the dataset (morphospace density), the median indicates the central  
328 position in the dataset (morphospace position; equivalent to the centroid in a  
329 multidimensional dataset), and the ranges quantify the amplitude of the variables  
330 (morphospace size). The presence of significant differences across the different time  
331 bins for the three disparity measures was determined by 95% confidence intervals  
332 calculated from 9,999 bootstrap replicates. All disparity metrics and resampling  
333 analyses were calculated in the R 4.0.2 software environment (R Core Team, 2020).

#### 334 **Palaeolatitudinal analyses**

335 To evaluate the relationship between body size and the palaeolatitudinal distribution of  
336 species, the dataset was divided into palaeolatitudinal bins. They were discretized using  
337 a cluster analysis based on the palaeolatitudinal coordinates of each reported specimen  
338 of each species in PAST 4.03 (Hammer *et al.*, 2001). Equivalent palaeolatitudes in the  
339 Southern and Northern Hemispheres were considered as part of the same bin with the  
340 aim of grouping similar global macroclimatic areas (*i.e.*, symmetrical temperature  
341 variation towards both poles). The cluster analysis recovered the following five pairs of  
342 palaeolatitudinal bins: 1) 19°N –19°S, 2) 19°–28°N and 19°–28°S, 3) 28°–47°N and  
343 28°–47°S, 4) 47°–80°S and 47°–80° N, and 5) >80°N and >80°S (Fig. 2).

344 Palaeolatitudinal analyses were performed for the same time bins described  
345 above. Species represented only by juvenile specimens, species whose femoral length  
346 could not be measured or estimated, and species present in more than one time bin  
347 because of their chronostratigraphic uncertainty were not considered. The median of the  
348 femoral length was calculated for each time bin and the presence of significant  
349 differences between them was determined by 95% confidence intervals calculated from  
350 9,999 bootstrap resampling replicates. The standard deviation and ranges were not

351 calculated for the palaeolatitudinal analyses because we wanted to explore the spatial  
352 distribution of body size through time, not the disparity. Phylogenetic Generalized Least  
353 Squares (pGLS) regressions between femoral length and the module of the raw  
354 palaeolatitudinal value of each species were performed for 100 randomly resolved trees  
355 for all the dataset and for less inclusive clades in both supertrees, respectively (see  
356 below). In particular, the regressions of the complete archosauromorph dataset  
357 (Permian–Early Jurassic) were performed for 1,000 randomly resolved trees, because of  
358 the larger number of possible alternative interrelationships that are expected in a broader  
359 taxonomic sample. The percentage of trees with significant correlations was calculated.  
360 Palaeocoordinates were plotted against femoral length and the linear function recovered  
361 for each of the 100 regressions (or 1,000 regressions in the case of the complete dataset)  
362 was added together with the phylogenetic relationships among species represented by  
363 one, randomly chosen, time-calibrated tree as a graphical example (Supplementary  
364 Online Information III). All these analyses were performed in the R 4.0.2 software  
365 environment (R Core Team, 2020), including the function gls() of the package nlme 3.1  
366 (Pinheiro *et al.*, 2020) for the pGLS regressions and the function phylomorphospace()  
367 of the package phytools 0.7-70 for the plot of the phylogeny in the biplots (Revell,  
368 2012).

### 369 **Supertree construction**

370 The pGLS regressions require temporally calibrated phylogenetic trees. As a  
371 consequence, we built two informal phylogenetic supertrees that included all the  
372 archosauromorph species sampled in the body size dataset. These informal supertrees  
373 were built using the tree editing tools of Mesquite 3.61 (Maddison & Maddison, 2019).  
374 Higher-level phylogenetic relationships were based on the hypotheses recovered by  
375 Nesbitt (2011) and Nesbitt *et al.* (2015) for one of the supertrees (hereafter called

376 ‘Nesbitt supertree’) and by Ezcurra (2016) for the other supertree (hereafter called  
377 ‘Ezcurra supertree’), which is a procedure that has been used in previous studies (*e.g.*,  
378 Grinham *et al.*, 2019; Fernandez Blanco *et al.*, 2020). Both hypotheses are largely  
379 consistent with one another, but differ in the phylogenetic position of some clades  
380 (Ezcurra *et al.*, 2021b; see Supplementary Online Information I). The use of both  
381 topologies allowed evaluating the sensitivity of the analyses to differences in the  
382 phylogenetic hypotheses.

383 In addition, other recently published phylogenetic hypotheses were used to  
384 include species or taxonomically less inclusive clades, the diversity of which were not  
385 widely sampled by Nesbitt (2011), Nesbitt *et al.* (2015) and Ezcurra (2016).  
386 Supplementary Online Information I details the use of these other phylogenetic  
387 hypotheses for particular supertree regions. In particular, *Prolacertoides jimusarensis*,  
388 “*Chasmatosuchus*” *vjushkovi*, and *Uralosaurus magnus* were excluded a priori from the  
389 supertrees because of their highly unstable phylogenetic positions (Ezcurra, 2016). The  
390 polytomies present in those original phylogenetic hypotheses were included in the  
391 supertrees. Topological inconsistencies between the different source hypotheses were  
392 taken into account by including polytomies that were consistent with the alternative  
393 phylogenetic positions in the original trees (see Goloboff & Pol, 2002: semi-strict  
394 supertree method). The two supertrees contain 376 middle Permian to Early Jurassic  
395 archosauromorph species or diagnostic specimens, hereafter referred to as ‘species’ for  
396 simplicity (Supplementary Online Information I).

397 **Temporal calibration of the supertrees**

398 Branch lengths were added to the two supertrees using “equal paleotree legacy” as a  
399 non-stochastic temporal calibration method (Brusatte *et al.*, 2008a; Bapst, 2012). The  
400 age of the root of the supertree was established before the calibration at 269.3 Ma,

401 following the age of the dichotomy between Archosauromorpha and  
402 Lepidosauromorpha proposed by Ezcurra *et al.* (2014). The calibration was performed  
403 with the timePaleoPhy() function of the R package paleotree 3.3.25 (Bapst, 2012).  
404 Species represented only by juvenile individuals or for which it was not possible to  
405 record the femoral length were used to calibrate the supertrees in order to consider their  
406 temporal information, but they were pruned from the trees for all other subsequent  
407 analyses (Supplementary Online Information III).

## 408 RESULTS

### 409 Body size disparity through time

410 **Archosauromorpha.** In the analysis of the entire dataset, it was found that the mean of  
411 the log-transformed femoral length (henceforth "log10(FL)") shows a general trend  
412 towards slightly higher values throughout the studied temporal range. There is a decline  
413 in the Olenekian and the highest value is reached in the Hettangian–Sinemurian (Fig.  
414 3.1). The upper limit of log10(FL) increases gradually from the Permian to the Early  
415 Jurassic. The lower limit is variable, but the highest values are observed in the Early  
416 Jurassic (with the exception of the Permian).

417 Regarding the variables that we used as measures of body size disparity (Fig.  
418 3.2–3.4), the standard deviation does not present significant differences between  
419 continuous time bins from the Permian to the late Carnian–early Norian, although the  
420 Anisian values are significantly higher than those of the middle–late Permian (this is not  
421 marked in the respective figure because only significant differences between  
422 consecutive time bins are indicated). The standard deviation increases significantly in  
423 the middle Norian–Rhaetian and then maintains similar values after the Triassic/Jurassic  
424 extinction. There is a non-significant increase of this variable in the Pliensbachian–  
425 Toarcian. The ranges show a trend towards higher values from the Permian to the

426 middle Norian–Rhaetian, but only in the latter interval a significant increase was  
427 recovered with respect to the previous time bins. After the Triassic/Jurassic boundary,  
428 the ranges decrease significantly and remain approximately constant until the end of the  
429 Early Jurassic. The median does not present significant differences between the studied  
430 time bins.

431 **Non-archosaurian Archosauromorpha (stem-Archosauria).** The mean  $\log_{10}(\text{FL})$   
432 remains constant across the Permian/Triassic boundary and subsequently decreases in  
433 the Olenekian (Fig. 4.1). After this stage, the mean increases progressively until the last  
434 interval in which the group is sampled (late Carnian–early Norian). The upper limit of  
435  $\log_{10}(\text{FL})$  remains approximately constant, but with a notable increase in the Anisian.  
436 The lower limit varies considerably, with its highest values in the Induan and Ladinian–  
437 early Carnian, respectively, with the exception of the poorly sampled Permian bin.

438 Regarding the disparity metrics (Fig. 4.2–4.4), there is a non-significant increase in the  
439 standard deviation from the Permian to the Olenekian, followed by a non-significant  
440 decrease until the late Carnian–early Norian. The ranges increase from the Permian to a  
441 peak in the Anisian, which is significantly higher than the Permian ranges.  
442 Subsequently, the ranges decrease significantly in the Ladinian–early Carnian and there  
443 is no significant difference in the last time interval. The median does not present  
444 significant differences between the studied time bins.

445 **Pseudosuchia.** The mean  $\log_{10}(\text{FL})$  maintains similar values from the Anisian to the  
446 Late Triassic, but then decreases considerably in the Early Jurassic (Fig. 5.1). The upper  
447 limit of  $\log_{10}(\text{FL})$  values increases after the Anisian, remaining almost constant until  
448 decreasing conspicuously in the Early Jurassic. The lower limit is more variable, with  
449 its highest values in the Anisian and middle Norian–Rhaetian, respectively. The lowest  
450 values of the lower limit are found in the late Carnian–early Norian and after the

451 Triassic/Jurassic boundary. Regarding the disparity metrics (Fig. 5.2–5.4), the standard  
452 deviation maintains similar values during the Triassic, with the exception of a non-  
453 significant increase in the Ladinian–early Carnian. By contrast, this variable decreases  
454 significantly in the Jurassic with respect to the middle Norian–Rhaetian value. The  
455 ranges show a trend towards higher values, although the changes between the Anisian  
456 and the late Carnian–early Norian are non-significant. Subsequently, the ranges  
457 decrease slightly and non-significantly in the middle Norian–Rhaetian, but they are  
458 significantly higher than in the Anisian (this is not marked in the respective figure  
459 because only significant differences between consecutive time bins are indicated). After  
460 the Triassic/Jurassic boundary, there is a significant decrease in the ranges. The median  
461 does not present significant variations during the Triassic, but it decreases significantly  
462 in the Early Jurassic, repeating the pattern observed in the other two disparity metrics.

463 **Non-dinosaurian Pan-Aves.** The mean  $\log_{10}(\text{FL})$  presents its highest value in the  
464 Anisian and subsequently decreases in the Ladinian–early Carnian. It maintains similar  
465 values up to the Early Jurassic, but with a slight decrease in the middle Norian–Rhaetian  
466 (Fig. 6.1). The upper limit of  $\log_{10}(\text{FL})$  has its maximum value in the Anisian and its  
467 lowest value in the Pliensbachian–Toarcian. The lower limit gradually decreases during  
468 the Triassic, and then rises in the Early Jurassic (both in the Hettangian–Sinemurian—  
469 which has only one taxon—and in the Pliensbachian–Toarcian). Among the body size  
470 disparity metrics (Fig. 6.2–6.4), the standard deviation increases in the late Carnian–  
471 early Norian and middle Norian–Rhaetian with respect to the previous intervals, but not  
472 significantly. Subsequently, it decreases, but not significantly, in the Early Jurassic. The  
473 ranges show similar variations to those of the standard deviation, but in this case the  
474 decrease in the Early Jurassic is significant. The median shows a pattern of decrease  
475 through the Triassic and then an increase in the Early Jurassic, but the differences are

476 not significant between continuous intervals. However, the medians of the middle  
477 Norian–Rhaetian and Pliensbachian–Toarcian are significantly lower than that of the  
478 Anisian (this is not marked in the respective figure because only significant differences  
479 between consecutive time bins are indicated).

480 **Sauropodomorpha.** The mean  $\log_{10}(\text{FL})$  of the sauropodomorphs increases  
481 conspicuously from their first appearance in the late Carnian–early Norian until the end  
482 of the Triassic. Subsequently, the values of this variable present a very gradual increase  
483 towards the end of the Early Jurassic (Fig. 7.1). The upper limit increases considerably  
484 up to the Hettangian–Sinemurian and maintains similar values in the Pliensbachian–  
485 Toarcian. The lower limit has its lowest values in the late Carnian–early Norian and  
486 Hettangian–Sinemurian. Regarding the disparity metrics (Fig. 7.2–7.4), the standard  
487 deviation and the ranges did not vary significantly during the Triassic and Early  
488 Jurassic. There is a significant increase in the median between the late Carnian–early  
489 Norian and the middle Norian–Rhaetian, which is followed by a gradual, but not  
490 significant, increase during the Early Jurassic.

491 **Theropoda.** The mean  $\log_{10}(\text{FL})$  remains relatively constant during the Late Triassic  
492 and increases in the Early Jurassic (Fig. 8.1). Both upper and lower limits of  $\log_{10}(\text{FL})$   
493 behave very similarly to the mean. No significant differences are observed over time in  
494 the body size disparity metrics (Fig. 8.2–8.4). The standard deviation increases slightly  
495 from the Late Triassic to the Early Jurassic, whereas the ranges decrease slightly from  
496 the Late Triassic to the Early Jurassic. The median remains relatively constant, but  
497 peaks immediately after the Triassic/Jurassic boundary.

498 **Ornithischia.** The mean  $\log_{10}(\text{FL})$  remains approximately constant through the studied  
499 time bins (Supplementary Online Information Fig. S3). The upper and lower limits of  
500  $\log_{10}(\text{FL})$  have their maximum values in the Hettangian–Sinemurian and then decrease

501 slightly in the Pliensbachian–Toarcian. None of the disparity metrics show significant  
502 variations over time (Supplementary Online Information Fig. S4). The standard  
503 deviation and ranges remain relatively constant during the Early Jurassic, whereas the  
504 median increases slightly during this interval.

505 **Body size disparity through time including species recorded in more than one time  
506 bin**

507 In this sensitivity analysis, the mean  $\log_{10}(\text{FL})$  shows a trend towards increase after the  
508 Early Triassic, but a pattern of decrease from the Permian to the Olenekian (Fig. 9.1).  
509 The upper limits also show a pattern of increase over time, including the Early Triassic.  
510 The lowest values of the lower limit are found in the Olenekian, Anisian, late Carnian–  
511 early Norian, and middle Norian–Rhaetian. The lower limits are considerably higher in  
512 the Early Jurassic than in the Late Triassic. In the case of the disparity metrics (Fig. 9.2–  
513 9.4), there is no significant difference between the standard deviations of consecutive  
514 time bins (the middle Norian–Rhaetian significant difference recovered above is lost).  
515 This disparity metric presents a pattern very similar to that described for the reduced  
516 dataset. The median possesses a pattern similar to that recovered in the original analysis,  
517 but with more conspicuous non-significant increases in both Early Jurassic time bins  
518 and a decrease in the Induan. Regarding ranges, the pattern is also generally congruent  
519 with that of the previous results, but there are significant increases in the Induan and the  
520 Olenekian. In the Late Triassic, there is also a significant increase of the ranges in the  
521 late Carnian–early Norian, contrasting with the significant increase seen in the middle  
522 Norian–Rhaetian in the reduced dataset. The significant decrease in ranges after the  
523 Triassic/Jurassic boundary is also found in this sensitivity analysis.

524 Particularly for the non-archosaurian archosauromorph grade the mean  
525  $\log_{10}(\text{FL})$  and the disparity metrics show a behaviour similar to that of the original

526 analysis. The main difference between the means is the recovery of an Induan value that  
527 is lower than that of the Permian and closer to that of the Olenekian. Regarding the  
528 disparity metrics, the increase in the ranges between the Permian and Induan is now  
529 recovered as significant. In this dataset, the sampling of non-archosaurian  
530 archosauromorphs could be extended into the middle Norian–Rhaetian time bin, but  
531 there is no significant difference with respect to the late Carnian–early Norian.

532 Other taxonomic groups (*i.e.*, Pseudosuchia, Sauropodomorpha, Theropoda, and  
533 Ornithischia) show very similar results to those obtained in the original analyses. In  
534 particular, the decrease of the standard deviation after the Triassic/Jurassic boundary  
535 and the increase of ranges in the late Carnian–early Norian became significant for the  
536 non-dinosaurian pan-avian grade.

### 537 **Palaeolatitudinal distribution of body size through time**

538 The medians between all the palaeolatitudinal bins were compared to one another for  
539 each time bin with representative data (*i.e.*, >5 archosauromorph species in at least two  
540 palaeolatitudinal bins). The temporal intervals that did not meet this requirement were  
541 the middle–late Permian (only two species present), Induan (only five species present),  
542 Olenekian (only five species, of which three were located in the 47°–80° bin), and  
543 Ladinian–early Carnian and Hettangian–Sinemurian (almost all species were present in  
544 the 28°–47° bin). In addition, analyses were performed on the dataset with  
545 archosauromorph species present in more than one time bin, but they did not yield  
546 different results from those of the original analysis.

547 In the Anisian, there are species present in four of the palaeolatitudinal bins. The  
548 mean log<sub>10</sub>(FL) has its maximum value in the bin that includes the palaeo-Equator and  
549 decreases in the 19°–28° bin (Fig. 10.1). However, the species sampling is very poor in  
550 these two palaeolatitudinal bins, being represented by five and two species, respectively.

551 The means corresponding to the 28°–47° and 47°–80° bins are quite similar between  
552 one another. As for the median, a significant increase in the 28°–47° palaeolatitudinal  
553 bin is recovered with respect to the 19°–28° bin (Fig. 10.2).

554 For the late Carnian–early Norian, there are species present in three of the  
555 palaeolatitudinal bins, but the area that corresponds to the 19°–28° bin is represented by  
556 a single species (Fig. 10.3). The mean  $\log_{10}(\text{FL})$  is higher in the bin that includes the  
557 palaeo-Equator than that corresponding to the 28°–47° bin (Fig. 10.4).

558 In the middle Norian–Rhaetian, there are species present in four of the  
559 palaeolatitudinal bins. The mean  $\log_{10}(\text{FL})$  has its maximum value in the 47°–80° bin  
560 (but only four species are present in this area), it decreases in the 19°–28° bin, and  
561 increases again in the palaeo-Equatorial belt (Fig. 10.5). The median  $\log_{10}(\text{FL})$  for the  
562 highest palaeolatitudinal bin is significantly higher than the median of all the other bins.  
563 By contrast, the median of the 19°–28° bin is lower than that of the other bins (Fig.  
564 10.6).

565 In the Pliensbachian–Toarcian, there are species present in only two of the  
566 palaeolatitudinal bins. The mean and median of the  $\log_{10}(\text{FL})$  are lower in the 19°–28°  
567 bin than in the 28°–47° bin, but the difference is not significant between medians  
568 (Supplementary Online Information Fig. S10).

#### 569 **Relationship between body size and palaeolatitude through time**

570 The following time bins were not considered for the pGLS regressions because of their  
571 low number of sampled species: middle–late Permian (only two species), Induan (only  
572 five species), and Olenekian (only five species). In addition, certain less inclusive  
573 groups were analysed or not depending on the available taxonomic sample of each time  
574 bin. The results recovered for both supertrees were very similar, varying slightly in the  
575 percentage of significant analyses found in the regressions.

576 In the Anisian, there is no significant correlation between body size and  
577 palaeolatitude in Archosauromorpha (Fig. 11.1). By contrast, there is a clear pattern of  
578 body size reduction towards higher palaeolatitudes in Pseudosuchia (Fig. 11.2).  
579 However, the latter result is not significant for the  $\log_{10}(\text{FL})$ ~palaeolatitude regressions  
580 and the same occurs for the other regressions in this time bin.

581 For the Ladinian–early Carnian, a slight increase in body size is observed  
582 towards higher palaeolatitudes for the complete dataset, but these regressions are not  
583 significant.

584 In the late Carnian–early Norian, there is a significant  $\log_{10}(\text{FL})$ ~palaeolatitude  
585 correlation that involves a body size reduction towards higher palaeolatitudes for 43%  
586 of the trees based on the ‘Ezcurra supertree’ and 47% of those based on the ‘Nesbitt  
587 supertree’ for the complete dataset (Fig. 11.3). If the data is restricted to Pseudosuchia  
588 and Phytosauria, respectively, the percentage of significant regressions increases to  
589 100% of the trees based on the ‘Ezcurra supertree’ and to 99% of the trees based on the  
590 ‘Nesbitt supertree’ (Fig. 11.4).

591 In the middle Norian–Rhaetian, there is a significant  $\log_{10}(\text{FL})$ ~palaeolatitude  
592 correlation showing a body size reduction towards higher palaeolatitudes for 89% of the  
593 trees for Pseudosuchia (Fig. S20) and for 100% of the trees for Crocodylomorpha (Fig.  
594 11.6) based on the ‘Ezcurra supertree’, and for 93% and 0% of the trees based on the  
595 ‘Nesbitt supertree’, respectively. The latter result of 0% significant correlations in the  
596 ‘Nesbitt supertree’ in comparison to the 100% significant correlations in the ‘Ezcurra  
597 supertree’ is probably related to the very low sampling of Crocodylomorpha ( $n=6$ ) in  
598 this interval. As a result, even minor differences in tree topology between both  
599 hypotheses seem to have strong consequences for the results. There are no significant

600 log<sub>10</sub>(FL)~palaeolatitude correlations for the complete dataset using the trees based on  
601 both supertrees (Fig. 11.5).

602 In analyses merging the data of all the Triassic time bins, there is a significant  
603 trend of body size reduction towards higher palaeolatitudes in Crocodylomorpha and  
604 Phytosauria. These results are supported by a significant log<sub>10</sub>(FL)~palaeolatitude  
605 correlation in 100% of the trees for Crocodylomorpha and in 70% of the trees for  
606 Phytosauria based on the ‘Ezcurra supertree’ (Fig. 12.1 and 12.2 respectively).

607 Regarding the trees based on the ‘Nesbitt supertree’, these significant regressions are  
608 recovered in 67% and 100% of the cases, respectively.

609 For the Hettangian–Sinemurian, there is a significant log<sub>10</sub>(FL)~palaeolatitude  
610 correlation of body size increase towards higher palaeolatitudes in 100% of the trees  
611 based on both supertrees using the complete dataset of this time bin (Fig. 13.1). In  
612 particular, we recovered a significant log<sub>10</sub>(FL)~palaeolatitude correlation with the  
613 same trend in 100% of the trees based on both supertrees for Theropoda.

614 In the Pliensbachian–Toarcian, there is a trend of body size reduction towards  
615 higher palaeolatitudes for all archosauromorphs, with a significant  
616 log<sub>10</sub>(FL)~palaeolatitude correlation in 84% of the trees based on the ‘Ezcurra  
617 supertree’ (Fig. 13.2) and 86% of the trees based on the ‘Nesbitt supertree’. However,  
618 this pattern disappears when subclades are analysed, without significant results for the  
619 trees derived from both supertrees.

620 Finally, in analyses of the entire archosauromorph dataset merging all time bins,  
621 there is a significant log<sub>10</sub>(FL)~palaeolatitude correlation of body size reduction  
622 towards higher palaeolatitudes in 30–40% of the trees in both supertrees (Figs. S57,  
623 S58).

624 **DISCUSSION**

625 **Body size disparity**

626 Archosauromorphs reached a high diversity of body sizes between their origin in the  
627 middle–late Permian and the Early Jurassic (the youngest time bin studied here),  
628 ranging from tiny pterosaurs such as *Arcticodactylus cromptonellus* (femoral length  
629 [FL] = 1.97 cm) to giant sauropodomorphs like *Barapasaurus tagorei* (FL = 136.5 cm).

630 The results of these analyses show that the dynamics of the body size disparity of  
631 Archosauromorpha during the first 90 million years of their evolution were complex.

632 The most remarkable pattern observed is an increase in their maximum size and their  
633 body size disparity from the Permian to the Late Triassic. After the Triassic/Jurassic  
634 boundary, the assemblage of lineages enclosed within the non-dinosaurian archosaur  
635 grades shows in average a decrease in their maximum body size and their body size  
636 disparity, whereas sauropodomorph dinosaurs show an increase of the same variables.

637 **Archosauromorpha.** In the Induan, the median has a slight increase with respect to the  
638 Permian value, because there is a concentration of larger species, although smaller  
639 species are also observed (Fig. 3.1). The standard deviation and ranges are also higher  
640 than in the Permian due to the presence of more disparate body sizes after the mass  
641 extinction event (Fig. 3.2–3.3). Nevertheless, it is important to consider that in the  
642 Permian only two archosauromorph species with femoral length measurements are  
643 recorded in our dataset. The decrease in mean log10(FL) in the Olenekian is driven by  
644 the appearance of small species, mainly by the non-archosaurian archosauromorph  
645 *Boreopricea funerea* (FL = 2.5 cm, Supplementary Online Information II). Indeed, the  
646 decrease in the median and the increase in the ranges and standard deviation with  
647 respect to the Induan are consistent with the presence of smaller species in the  
648 Olenekian. In the Anisian, the lower limit of log10(FL) retains a similar value because  
649 of the persistence of relatively small species, such as the non-crocopodan *Pectodens*

650 *zhenyuensis* (FL = 3.2 cm, Supplementary Online Information II). In contrast, the upper  
651 limit increases considerably because of the appearance of pseudosuchians and  
652 erythrosuchids with femoral lengths between 45–50 cm (Supplementary Online  
653 Information II), which is consistent with what was recovered by Sookias *et al.* (2012b)  
654 and Turner and Nesbitt (2013) for this time interval. This pattern is also indicated by an  
655 increase in the median and ranges during the Anisian with respect to the Induan values,  
656 but the standard deviation decreases because there is a lower internal variation in the  
657 dataset due to a concentration of numerous medium-sized species with femoral lengths  
658 between 14–30 cm (Fig. 3.2–3.4). In the Ladinian–early Carnian, the upper limit of  
659  $\log_{10}(\text{FL})$  continues to increase due to the presence of large pseudosuchians, such as  
660 *Luperosuchus fractus* (estimated FL = 78 cm, Supplementary Online Information II).  
661 However, the levels of disparity remain similar to those of the previous time bin,  
662 because there is also an increase in the lower limit due to the disappearance of small  
663 species. In the late Carnian–early Norian, the decrease in the lower limit of  $\log_{10}(\text{FL})$  is  
664 interpreted as a result of the reappearance of small species, mainly non-dinosaurian pan-  
665 avians, leading to a slight increase in the ranges. There is also a high concentration of  
666 medium to large-sized species, mainly driven by pseudosuchians (various aetosaurs and  
667 phytosaurs) and the oldest known dinosaurs, which is reflected in the disparity metrics  
668 as a slight decrease in the standard deviation and increase in the median.

669 By the end of the Triassic, in the middle Norian–Rhaetian, the significant  
670 increase in the ranges is produced by an increase in the upper limit of  $\log_{10}(\text{FL})$ ,  
671 accompanied by a decrease of its lower limit (Fig. 3.1–3.3). The upper limit increases to  
672 levels that have not been reached previously by the clade—not even by large Anisian to  
673 Ladinian–early Carnian pseudosuchians—because of the appearance of large  
674 saurodromorphs, such as *Ingentia prima* and *Camelotia borealis* (FL >100 cm),

675 whereas the lower limit decreases because of the presence of small pterosaurs. There are  
676 also significant differences in the standard deviation, which increases due to the  
677 presence of a greater internal variation due to the presence of disjoint sizes as those  
678 previously mentioned and also a smaller proportion of medium-sized species. The  
679 median increases slightly because of the presence of the large sauropodomorphs (Fig.  
680 3.4).

681 After the Triassic/Jurassic boundary, the significant decrease in the ranges in the  
682 Hettangian–Sinemurian is as a result of an increase in the lower limit of  $\log_{10}(\text{FL})$   
683 because of the disappearance of relatively small species (all species with  $\text{FL} < 6.6 \text{ cm}$ ,  
684 Supplementary Online Information II). Despite the disappearance of these small species,  
685 the standard deviation remains approximately constant after the boundary because of the  
686 absence of medium-sized species ( $\text{FL} = 28\text{--}40 \text{ cm}$ , Supplementary Online Information  
687 II). In the Pliensbachian–Toarcian, the youngest time bin sampled here, some small  
688 pterosaur species occur and lead to a decrease in the lower limit of  $\log_{10}(\text{FL})$  and a non-  
689 significant increase of the ranges. The high upper limit is maintained by the presence of  
690 large sauropodomorph dinosaurs. The standard deviation increases because of the  
691 presence of a disjoint structure of body sizes, as in the previous time bin.

692 In summary, the general pattern observed for archosauromorphs is an increase in  
693 their maximum size and their body size disparity from the Permian to the Late Triassic,  
694 as previously observed by Turner and Nesbitt (2013). This maximum size was  
695 maintained during the Early Jurassic, but the lower limit of the body size was deeply  
696 affected by the Triassic/Jurassic mass extinction, as a result of the disappearance of  
697 relatively small species.

698 In analyses including species belonging to more than one time bin due to  
699 chronostratigraphic uncertainty (Fig. 9), the mean and median decrease in the Induan

700 compared to the original analysis because of the inclusion of small species dated as  
701 Induan–Olenekian, such as the non-archosauriform crocodylomorphs *Prolacerta broomi* and  
702 *Teyujagua paradoxa*. The loss of the significant increase in the standard deviation in the  
703 middle Norian–Rhaetian time bin occurs due to the addition of numerous species that  
704 are also present in the late Carnian–early Norian, decreasing the internal variation of the  
705 datasets. In the Early Jurassic, there are more conspicuous increases in the mean  
706 because of the inclusion of several large sauropodomorph species (*e.g.*, *Barapasaurus*  
707 *tagorei*, *Kotasaurus yamanpalliensis*, *Tonganosaurus hei*) with poor chronostratigraphic  
708 resolution.

709 The major difference between both analyses is observed in the ranges (Fig. 9.3).  
710 Although they show an overall similar pattern, in the secondary analysis we have  
711 significant increases from the Permian to the Induan and from the Induan to the  
712 Olenekian. In the first case, this is because of the inclusion of small species (*e.g.*,  
713 *Prolacerta broomi*, *Teyujagua paradoxa*) and in the second due to the presence of  
714 relatively large species, such as the poposauroid pseudosuchian *Xilousuchus*  
715 *sapingensis* (estimated FL = 30.2 cm, Supplementary Online Information II). The  
716 continuous increase of the ranges during the Triassic is also recovered, but a significant  
717 difference is seen in the late Carnian–early Norian, rather than in the middle Norian–  
718 Rhaetian, which is exemplified by the presence of the sauropodomorph *Ruehleia*  
719 *bedheimensis* (FL = 80 cm) and the pterosaur *Arcticodactylus cromptonellus* (FL = 1.97  
720 cm) as the most marginal species.

721 **Non-archosaurian Archosauromorpha.** The results for the taxa included within this  
722 paraphyletic group are the same as for the entire dataset in the first three time bins (*i.e.*,  
723 Permian to Olenekian) (Fig. 4). The maximum sizes documented occur during the  
724 Anisian (Fig. 4.1), increasing the upper limit of log<sub>10</sub>(FL), and correspond to the

725 erythrosuchids, such as *Erythrosuchus africanus* (FL = 46.6) and *Shansisuchus*  
726 *shansisuchus* (estimated FL = 34.4 cm) (Supplementary Online Information II). The  
727 lower limit of the Anisian also increases, but to a lower degree, because there are  
728 several smaller species. As a result, the range increases slightly, but the standard  
729 deviation decreases due to the presence of numerous species of intermediate sizes, such  
730 as the non-archosauriform archosauromorphs *Dinocephalosaurus orientalis* (FL =  
731 11.62) and *Pamelaria dolichotrachela* (FL = 16.45) (Fig. 4.2–4.3).

732 In the Ladinian–early Carnian, both the upper and lower limits of body size are  
733 reduced, with more medium-sized forms present, with only femoral lengths between 6–  
734 25 cm observed. This generates a decrease in both standard deviation and ranges, a  
735 pattern that has not been recovered in a previous analysis focused on the South  
736 American sample of non-archosaurian archosauromorphs (Ezcurra *et al.*, 2021c). In the  
737 youngest sampled interval, the late Carnian–early Norian, the standard deviation  
738 continues to decrease as a result of a lower internal variation in the dataset and the  
739 median increases (Fig. 4.4). This is because the group is restricted to specialized  
740 medium-sized forms, such as *Trilophosaurus buettneri* and rhynchosauroids (*e.g.*,  
741 *Hyperodapedon*, *Teyumbaita*), prior to their extinction. However, the ranges increase  
742 mainly because of the presence of a single relatively small species, the proterochampsid  
743 *Cerritosaurus binsfeldi*. Non-significant increases have been reported for the three  
744 metrics during the late Carnian–early Norian for the South American taxa within the  
745 non-archosaurian archosauromorph grade (Ezcurra *et al.*, 2021c), thus partially  
746 matching the global pattern.

747 **Pseudosuchia.** The oldest pseudosuchians in our femoral length dataset are Anisian in  
748 age. These species are mainly medium to small-sized, with the exception of the  
749 poposauroids *Arizonasaurus babbitti* and *Qianosuchus mixtus*, which have femoral

750 lengths of ca. 49 cm. In the subsequent interval, Ladinian–early Carnian, the increase in  
751 ranges is a result of the appearance of larger species, such as the ‘rauisuchian’  
752 *Luperosuchus fractus* and of small species (e.g., *Gracilisuchus stipanicicorum*, FL ~8  
753 cm, Supplementary Online Information II) (Fig. 5.3). The standard deviation also  
754 increases due to the presence of large loricatan predators and smaller forms belonging to  
755 other pseudosuchian clades (Fig. 5.2).

756 In the late Carnian–early Norian there is a large concentration of medium to  
757 large-sized species because of an abundance for the first time of aetosaurs and  
758 phytosaurs, in addition to the non-crocodylomorph loricatans already recorded in the  
759 previous time bin. This results in a decrease of the standard deviation, but not in the  
760 ranges, which increase. The latter is because the upper limit of log10(FL) remains  
761 similar to that during the Ladinian–early Carnian, but the lower limit decreases because  
762 of the presence of small species, such as *Erpetosuchus granti* (estimated FL = 5.9 cm,  
763 Supplementary Online Information II) (Fig. 5.1).

764 The ranges decrease during the middle Norian–Rhaetian. Although several  
765 crocodylomorph species with sizes smaller than those of other pseudosuchians appear in  
766 this time, there are not very small forms such as those reported in previous time bins  
767 (e.g., *Erpetosuchus granti*). For this same reason, there is an increase in the standard  
768 deviation, depicting a greater internal variation due to the presence of these small-sized  
769 crocodylomorphs.

770 After the Triassic/Jurassic boundary, the large decrease in the mean log10(FL)  
771 during the Hettangian–Sinemurian and the significant decrease of the three disparity  
772 metrics are caused by the extinction of all pseudosuchian groups with the exception of  
773 the crocodylomorphs (Fig. 5). The currently available fossil record shows that

774 pseudosuchians became restricted to crocodylomorphs with femoral lengths lower than  
775 16 cm after the mass extinction event.

776 **Non-dinosaurian pan-avians.** The oldest body fossil records of the taxa included  
777 within this paraphyletic group are Anisian in age and are represented by medium to  
778 small-sized forms, with femoral lengths between 10–18 cm and an indeterminate  
779 silesaurid with a considerably larger femoral length estimated in 34.5 cm (Barrett *et al.*,  
780 2015) (Supplementary Online Information II). Three species recorded in the Ladinian–  
781 early Carnian, there are only one lagerpetid and two dinosauriforms, the largest of  
782 which (*Lewisuchus admixtus* with a FL = 11.5 cm, Supplementary Online Information  
783 II) is similar in size to the smallest taxon of the previous time bin. As a consequence, a  
784 decrease in the mean log<sub>10</sub>(FL) is recovered during the Ladinian–early Carnian (Fig.  
785 6.1). The other body size disparity metrics also decrease because the few species  
786 recorded in this bin are all medium to small-sized, reducing the internal variation and  
787 ranges of the dataset (Fig. 6.2–6.3).

788 In the late Carnian–early Norian, there are larger (silesaurids) and smaller  
789 species (some lagerpetids) than in the previous interval. This results in an increase in the  
790 three body size disparity metrics (Fig. 6.2–6.4) for the assemblage of taxa enclosed in  
791 this paraphyletic group. The non-significant decrease in the median in the following  
792 interval, middle Norian–Rhaetian, is as a consequence of the appearance of very small  
793 pterosaurs (femoral length < 8.5 cm).

794 In the Early Jurassic, only pterosaurs survive of all these groups and they have  
795 larger sizes than their Triassic representatives. However, Early Jurassic pterosaurs  
796 reached shorter femoral lengths than Triassic silesaurids and most lagerpetids. As a  
797 result, there is a decrease in the standard deviation due to the concentration of species  
798 with femoral lengths between 4–9 cm, and a significant decrease in the ranges because

799 of a decrease of the upper limit of  $\log_{10}(\text{FL})$ —in which the longest FL decreased from  
800 21 cm to 8.72 cm)—and an increase in the lower limit due to the increase of the  
801 minimum body size of pterosaurs. It should be noted that only one species of pterosaur  
802 could be included in the Hettangian–Sinemurian interval because of the extremely poor  
803 record of this group during this time bin. As a consequence, the comparison between the  
804 body size disparity variables around the Triassic/Jurassic boundary have been restricted  
805 between the middle Norian–Rhaetian and the Pliensbachian–Toarcian time bins.

806 The significant decrease of the standard deviation after the Triassic/Jurassic  
807 boundary and the significant increase of ranges in the late Carnian–early Norian  
808 recovered among all the non-dinosaurian pan-avian groups after the inclusion of species  
809 present in more than one time bin are likely due to an increase of the statistical  
810 sensitivity of the analyses by the increase of the number of species in the sample size  
811 (Fig. S8).

812 **Dinosauria.** As reported before, sauropodomorphs exhibit a significant increase of the  
813 median of  $\log_{10}(\text{FL})$  in the Late Triassic, whereas the other disparity variables also  
814 show an increase, although non-significant, during this time span (Fig. 7). The latter is  
815 because although the upper limit of body size increases due to the appearance of very  
816 large species, such as *Ingentia prima*, the lower limit also increases due to the  
817 disappearance of relatively small species (e.g., non-bagualosaurian sauropodomorphs).  
818 Sauropodomorphs reached larger body sizes during the Early Jurassic, with a slight  
819 increase in the median and a decrease in the ranges during the Pliensbachian–Toarcian  
820 because of the absence of medium to small-sized forms (all species have  $\text{FL} > 76 \text{ cm}$ ,  
821 with the exception of *Seitaad ruessi* with an estimated  $\text{FL} = 32.65 \text{ cm}$ , Supplementary  
822 Online Information II).

823 In Theropoda, although no significant differences were observed (Fig. 8), the  
824 most notable is an increase in the median in the Hettangian–Sinemurian interval caused  
825 by the presence of some large species, such as *Sinosaurus triassicus*, *Dracovenator*  
826 *regenti* and *Tachiraptor admirabilis* (all with FL = 59–65 cm, Supplementary Online  
827 Information II).

828 In the case of ornithischians, *Pisanosaurus mertii* is the only Triassic member of  
829 the clade (Desojo *et al.*, 2020b; but see Agnolin & Rozadilla, 2017 and Baron *et al.*,  
830 2017 for an alternative interpretation as a silesaurid), which has an estimated femoral  
831 length of 17 cm. Early Jurassic ornithischians have a broad range of sizes, with very  
832 small species (*e.g.*, *Manidens condorensis*, estimated FL = 5.42 cm, Supplementary  
833 Online Information II) and relatively large forms (*e.g.*, *Scelidosaurus harrisonii*, FL =  
834 40.3 cm). The absence of significant or appreciable changes in the body size disparity  
835 metrics within the Early Jurassic is probably a consequence of the low number of  
836 ornithischian species currently known for this time span, which hampers detecting  
837 statistically significant differences.

838 **The impact of mass extinctions on the evolution of archosauromorph body size**  
839 **Permian/Triassic mass extinction.** None of the body size disparity metrics show  
840 significant changes between the Permian and the Induan in the analyses with species  
841 restricted to a single time interval. Nevertheless, significant changes were detected after  
842 adding species present in more than one time interval (Fig. 9). These significant  
843 changes, present in Archosauromorpha and the lineages included within the  
844 paraphyletic assemblage of non-archosaurian archosauromorphs, reveal that body size  
845 disparity increased after the Permian/Triassic boundary. The significant increase in the  
846 body size ranges of Induan archosauromorphs in the secondary analysis is as a result of  
847 an increase in the number of species in this interval that may have also been present in

848 the Olenekian, but not in the Permian. It is worth mentioning that these occurrences in  
849 more than one time interval are due to chronostratigraphic uncertainty and not because  
850 of a real presence of the taxa in both time intervals (*i.e.*, the species included in this  
851 analysis in the Induan could actually be exclusive to the Olenekian, the other way  
852 round, or belong to both bins). As a consequence, although the significant increase in  
853 the ranges with respect to the Permian values seems to be a robust result, it cannot be  
854 determined if it occurred in the Induan or in the Olenekian. The internal variation of the  
855 dataset also increases after the mass extinction, which is a consistent result with the  
856 significant increase in body size range. This increase is not significant between the  
857 Permian and Induan, but it is significant between the Permian and the Olenekian.

858 Turner and Nesbitt (2013) did not analyse quantitatively the evolution of  
859 archosauromorph body size around the Permian/Triassic boundary, but they mentioned  
860 that the body sizes of diapsids (not only of archosauromorphs) were smaller in the  
861 Palaeozoic than in the Mesozoic. This agrees with the results that we have recovered for  
862 archosauromorphs if we observe the behaviour of the upper limit of  $\log_{10}(\text{FL})$  for  
863 Archosauromorpha (Fig. 3.1). Nevertheless, the most conspicuous increase in the upper  
864 limit of body sizes occurs in the Anisian, several millions of years after the mass  
865 extinction event, while during the Early Triassic the maximum values increase very  
866 slightly. Our results are also consistent with those reported by Bernardi *et al.* (2015),  
867 who analysed the body size variation of archosauromorphs based on ichnofossils from  
868 Permo-Triassic sequences in Europe. These authors found an increase in the maximum  
869 and minimum limits of body sizes between the late Permian and the Early Triassic, but  
870 not a significant difference between the means at both sides of the Permian/Triassic  
871 boundary.

872 Regarding a more general pattern of palaeolatitudinal distribution of species, it is  
873 interesting to mention that the highest proportion of species in the Induan–Olenekian  
874 included in our data is found in the third palaeolatitudinal belt ( $28^{\circ}$ – $47^{\circ}$ ). This could be  
875 as a consequence of a preservation or sampling bias but, in particular, no species were  
876 recorded at low palaeolatitudes for the Early Triassic bin. Sun *et al.* (2012) concluded  
877 that the global temperature increased considerably after the Permian/Triassic boundary  
878 based on observed variations of the  $^{13}\text{C}$  and  $^{18}\text{O}$  isotope curves. These authors  
879 concluded that this change in global temperature may explain the scarce vertebrate  
880 record (including archosauromorphs) in equatorial zones around the Permian/Triassic  
881 boundary because these became probably uninhabitable. Sun *et al.* (2012) interpreted  
882 that the recovery of the equatorial fauna would have occurred in the Middle Triassic.  
883 Thus, our results are consistent with the hypothesis that the re-invasion of the equatorial  
884 zones would have occurred later than in higher palaeolatitudes (Payne *et al.*, 2004;  
885 Grauvogel-Stamm & Ash, 2005; Whiteside & Ward, 2011; Irmis & Whiteside, 2012;  
886 Sun *et al.*, 2012).

887 **Triassic/Jurassic mass extinction.** The analysis of the entire dataset shows that  
888 archosauromorphs reached their highest body size disparity before the Triassic/Jurassic  
889 boundary (Fig. 3) due to the co-occurrence of large sauropodomorphs and very small  
890 pterosaurs, as previously mentioned. After this boundary, whereas the standard  
891 deviation and the median remain at similar pre-extinction levels, the ranges decrease  
892 significantly and this reflects a retraction of the size-space occupation. Pseudosuchians  
893 and lineages included among the non-dinosaurian pan-avians were the most affected by  
894 the Triassic/Jurassic mass extinction, and this is clearly reflected in their body size  
895 disparity plots (Figs. 5, 6). In this regard, several decreases, some of them significant,  
896 are recovered in the disparity metrics, especially in Pseudosuchia. After the

897 Triassic/Jurassic boundary, pterosaurs and crocodylomorphs are represented by medium  
898 to small-sized forms, while dinosaurs are the only ones that record large forms. This  
899 suggests that pseudosuchians and most of the lineages enclosed within the non-  
900 dinosaurian pan-avian grade were strongly affected by the extinction event and that  
901 body size could have been a determining factor in their negative selection. In the case of  
902 pterosaurs, the only group of non-dinosaurian pan-avians to survive the Triassic/Jurassic  
903 mass extinction, other intrinsic factors, such as their ability to fly and/or their  
904 postcranial pneumatization related to the ventilatory system (O'Connor, 2006; Butler *et*  
905 *al.*, 2009), could have also played key roles. Sauropodomorphs and theropods (Figs. 7,  
906 8) seem to not have been negatively affected by the mass extinction, but conversely they  
907 increased their body size after the Triassic/Jurassic boundary. Olsen *et al.* (2002)  
908 analysed the ichnological evidence and corporeal remains of Triassic and Jurassic  
909 theropods and proposed the presence of a large increase in their body size in a short  
910 period of time near the Triassic/Jurassic boundary. Although we recover an increase in  
911 body size for Theropoda in the Hettangian–Sinemurian, we do not find it as a significant  
912 change. As a consequence, our results do not provide statistical support for the  
913 observations of Olsen *et al.* (2002). In the case of Ornithischia, the effect of the mass  
914 extinction cannot be analysed because their Triassic record is, at best, restricted to a  
915 single species.

916 Our results are consistent with those found by Turner and Nesbitt (2013), who  
917 recovered an increase of body size in the main three dinosaur clades and in pterosaurs,  
918 together with a decrease in the body size of crocodylomorphs, after the Triassic/Jurassic  
919 boundary. Turner and Nesbitt (2013) did not analyse the non-dinosaurian and non-  
920 pterosaurian pan-avian species (*e.g.*, Lagerpetidae, Silesauridae). These groups include  
921 several species with larger sizes than those of pterosaurs and contributed to a higher

922 body size disparity during the Triassic (Barrett *et al.*, 2015; Beyl *et al.*, 2020), which is  
923 lost in the Early Jurassic due to their disappearance in or slightly before the mass  
924 extinction event. Turner and Nesbitt (2013) also recovered a decrease in the body size  
925 of pseudosuchians after the Triassic/Jurassic boundary, which is a result that we also  
926 find here, together with a decrease in the body size disparity metrics.

927 In conclusion, the Triassic/Jurassic mass extinction would have selectively  
928 affected many groups of archosauromorphs, but the body size of dinosaurs, pterosaurs,  
929 and crocodylomorphs would not have been significantly affected. This pattern could  
930 also be seen as a negative selection that affected all medium to large-sized  
931 archosauromorph species, with the exception of dinosaurs. Allen *et al.* (2019) found no  
932 correlation between the mass extinction event and archosauromorph body size, although  
933 they leave open the possibility that there may have been a phylogenetic selection. Either  
934 way, for some reason, dinosaurs were the only archosauromorphs that retained the  
935 medium to large sizes already reached during the Late Triassic. The explanation for this  
936 macroevolutionary pattern goes beyond the objectives of this contribution, but it seems  
937 to have been the result of a condition intrinsic to dinosaurs, such as the presence of one  
938 or more apomorphies (*e.g.*, erect bipedal locomotion, possible presence of  
939 intergumentary structures) that allowed the group to continue the diversification that  
940 began before the Triassic/Jurassic mass extinction (Ezcurra, 2010b).

941 **Relationship between body size and palaeolatitudinal distribution**

942 In the Anisian dataset, the only significant difference is an increase in body size for the  
943 entire dataset towards higher palaeolatitudinal bins in the medians plot (Fig. 10.2),  
944 which is consistent with what would be expected for the Bergmann's Rule. However, we  
945 consider that this result is not robust because one of the bins has only two sampled  
946 species. The largest body sizes in this interval are those of pseudosuchians found in the

947 most equatorial belt and some medium to large-sized pseudosuchians and non-  
948 archosaurian archosauromorphs that have been collected at palaeolatitudes between  
949 47°–80°. Moreover, in the pGLS regressions, we obtained a trend of reduction of body  
950 sizes towards higher palaeolatitudes for pseudosuchians, but this is not significant.

951 For the late Carnian–early Norian, there are several medium to large-sized  
952 pseudosuchians (mainly phytosaurs) at low latitudes, whereas at high latitudes only a  
953 few species reach large sizes (some pseudosuchians and *Herrerasaurus*  
954 *ischigualastensis*). The main difference between these two bins is the absence of smaller  
955 species in the more equatorial belt, which produces a significant increase in body size  
956 towards lower latitudes in the median analyses. This matches the significant reduction  
957 of body sizes towards higher palaeolatitudes for pseudosuchians and phytosaurs found  
958 in the pGLS regressions (Fig. 11.4). These results disagree with what is proposed by  
959 Bergmann's Rule.

960 In the middle Norian–Rhaetian, there are significant increases in the body size  
961 median in the lower (0°–19°) and third (28°–47°) palaeolatitudinal belts with respect to  
962 the second one (19°–28°). This result is mainly driven by the occurrence of multiple  
963 large phytosaur species at low palaeolatitudes and sauropodomorphs in the third belt  
964 (pseudosuchians in the third belt are medium-sized species). By contrast, in the second  
965 palaeolatitudinal bin we have only pterosaurs (in addition to a marine phytosaur), which  
966 are smaller in size than the species of the other two bins. The pGLS regressions found a  
967 significant trend of body size reduction towards higher palaeolatitudes for  
968 pseudosuchians as a whole and for crocodylomorphs (Fig. 11.6). The pGLS results are  
969 more robust because the subclades are analysed separately and in an explicit  
970 phylogenetic context, whereas in the analysis of the medians the significant results are  
971 produced mainly by the presence of pterosaurs in the second palaeolatitudinal belt.

972 Thus, the latter result seems to reflect deep divergences in the biogeographic history of  
973 lineages with different average sizes (*e.g.*, pterosaurs versus pseudosuchians). As a  
974 result, we conclude that the results of the middle Norian–Rhaetian dataset matches a  
975 Converse Bergmann’s Rule pattern for pseudosuchians as a whole and particularly for  
976 crocodylomorphs.

977 These differences among palaeolatitudinal belts during the middle Norian–  
978 Rhaetian could be a consequence of intrinsic (*e.g.*, phylogenetic) or extrinsic (*e.g.*,  
979 palaeolatitudinal variations of the thermal gradient) factors, or a combination of both.  
980 Only a few groups of low taxonomic level are represented by several species in both  
981 low and high palaeolatitudes for the analysed time intervals. One of these are the  
982 pseudosuchians, in which larger species occur at lower palaeolatitudes in both the late  
983 Carnian–early Norian and the middle Norian–Rhaetian time bins. As recovered in the  
984 pGLS regressions including the complete Triassic dataset, the body size of phytosaurs  
985 and crocodylomorphs decreases significantly towards higher palaeolatitudes and this  
986 pattern may indicate a palaeolatitudinal influence on the body size of the clades. By  
987 contrast, this pattern is not recovered in aetosaurs (Supplementary Online Information  
988 Fig. S29) and this group in the southern hemisphere is mainly restricted to South  
989 America, whereas the record of phytosaurs in the southern hemisphere is mainly  
990 restricted to India. This pattern is not recovered in other studied groups; conversely,  
991 there is a significant trend of increase of body size towards higher palaeolatitudes for  
992 Theropoda in the earliest Jurassic, but this result is poorly supported because  
993 *Tachiraptor admirabilis* seems to represent an outlier. Thus, the pattern of body size  
994 reduction towards higher palaeolatitudes recovered in the pGLS regressions for the  
995 complete archosauromorph dataset of all studied time bins (Permian–Early Jurassic)

996 seems to be mainly driven by the patterns observed in Pseudosuchia (especially  
997 Phytosauria and Crocodylomorpha).

998 Our results indicate that variations in body size probably occur in at least some  
999 taxonomically restricted groups and there is some degree of body size structuring, either  
1000 as a consequence of palaeolatitudinal endemism in different taxonomic groups (Ezcurra,  
1001 2010a) and/or physiological factors (e.g., those related to a Converse Bergmann's Rule).  
1002 Moreover, our results also support the results found by Dunne *et al.* (2020) and  
1003 Stockdale and Benton (2021) (but see Benson *et al.*, 2021 for critical assessment of this  
1004 paper, in addition to having some contradictory results), who found evidence that  
1005 environmental factors influenced the taxonomic diversity and body size of  
1006 pseudosuchians, respectively.

1007 Bergmann's Rule was formulated for homeothermic animal species and there is  
1008 currently no consensus about the type of metabolism of Triassic archosauromorphs.  
1009 Most of the studies about this topic in Archosauromorpha are restricted to dinosaurs  
1010 (Benton, 1979; Grellet-Tinner, 2006; Grady *et al.*, 2014), but recently Cubo and Jalil  
1011 (2019) proposed that Triassic archosauromorphs would have been mostly endothermic  
1012 forms, including the phytosaur "*Rutiodon*" *carolinensis*, based on palaeohistological  
1013 data (Cubo & Jalil, 2019). Similarly, Seymour *et al.* (2004) concluded that not only  
1014 stem-crocodylians would have been endothermic, but also at least some stem-  
1015 archosauromorphs. These authors proposed that ectothermic forms would have evolved  
1016 from endothermic ancestors within Archosauromorpha. However, the results found here  
1017 for Pseudosuchia (especially Phytosauria and Crocodylomorpha) seems more consistent  
1018 with what would be expected for ectothermic animals, because the clade seems to have  
1019 reached their largest sizes at lower palaeolatitudes. This is congruent with the results  
1020 recovered by Dunne *et al.* (2020), where a greater richness of pseudosuchian species

1021 occurs in palaeoclimatic ranges restricted to warm environments. Low-latitude species  
1022 would have benefited from higher temperatures that allowed them to achieve higher  
1023 metabolic activity and body sizes, as it is observed in current ectothermic reptiles  
1024 (Makarieva *et al.*, 2005; Head *et al.*, 2009; Rodrigues *et al.*, 2018). Although several  
1025 medium to large-sized species of other pseudosuchians and non-archosaurian  
1026 archosauromorphs are also found at low palaeolatitudes, a larger sample of species is  
1027 required to test these hypotheses for these groups.

1028 As a result of recovering significant pGLS regressions between body size and  
1029 palaeolatitude for pseudosuchians, we conducted an additional analysis using the  
1030 residuals of these regressions. The analysis of these residuals allows us to determine if  
1031 the body size disparity patterns recovered for pseudosuchians were driven by the  
1032 palaeolatitudinal distribution of species (*e.g.*, if Late Triassic species were significantly  
1033 larger than Early Triassic species because they occurred at lower palaeolatitudes). The  
1034 three body size disparity metrics (*i.e.*, standard deviation, ranges and median) calculated  
1035 with the residuals of the  $100 \log_{10}(\text{FL})$ -palaeolatitude pGLS regressions for both  
1036 supertrees and both Triassic and Triassic-Early Jurassic pseudosuchians show the same  
1037 pattern as those calculated with the original dataset. Thus, we can conclude that the  
1038 palaeolatitudinal distribution of species fails to explain and did not drive the  
1039 macroevolutionary pattern of body size disparity recovered in pseudosuchians.

## 1040 CONCLUSIONS

1041 The results of the analyses conducted here allowed us to explore the evolutionary  
1042 dynamics of the archosauromorph body size during the first 90 million years of their  
1043 diversification. Our dataset allows rejection of the hypothesis that the Permian/Triassic  
1044 mass extinction did not produce significant changes in archosauromorph body size. This  
1045 hypothesis is rejected by the analysis that includes species present in more than one

1046 time bin. Thus, it is not possible to determine here if the increase of body size after the  
1047 Permian/Triassic mass extinction occurred shortly after the biotic crisis or later in the  
1048 Olenekian.

1049 Our analyses do not reject the hypothesis that the Triassic/Jurassic mass  
1050 extinction produced significant changes in the body size of pseudosuchian archosaurs.  
1051 Indeed, a significant decrease of body size is recovered in the Hettangian–Sinemurian  
1052 for this group. By contrast, we reject the hypothesis that the Triassic/Jurassic mass  
1053 extinction did not produce significant changes in the body size of pan-avian archosaurs.  
1054 Although dinosaurs do not undergo significant changes, the lineages enclosed within the  
1055 non-dinosaurian pan-avian grade, represented only by pterosaurs in post-Triassic times,  
1056 show significant changes.

1057 There is no general trend consistent with the hypothesis that the largest  
1058 archosauromorphs are found in localities positioned at higher palaeolatitudes and, thus,  
1059 this hypothesis is rejected. Although there are a few cases that may follow Bergmann's  
1060 Rule (*e.g.*, Hettangian–Sinemurian theropods in the pGLS regressions), they are not  
1061 well supported, and several others (*e.g.*, Late Triassic pseudosuchians in the pGLS  
1062 regressions) show a significant opposite pattern that is more consistent with  
1063 observations in several extant ectothermic animals.

1064 Matching macroevolutionary patterns are obtained for Pseudosuchia and the  
1065 lineages included within the non-dinosaurian pan-avian grade before and after the  
1066 Triassic/Jurassic mass extinction, in which medium to large-sized species became  
1067 extinct, with only the relatively small-sized crocodylomorphs and pterosaurs surviving  
1068 the extinction, respectively. This biotic crisis does not appear to have affected dinosaurs  
1069 significantly, which continued to increase their sizes in the Early Jurassic. This evidence  
1070 suggests that some variables must have prevented the negative selection of medium to

1071 large-sized dinosaurs during the mass extinction event, such as one or more apomorphic  
1072 character states related to their palaeophysiology (e.g., integument isolation) and/or  
1073 palaeoecology (e.g., locomotion).

1074 A structuring of the body size is observed in the analyses comparing  
1075 palaeolatitudinal bins, which show that body size may have a more complex co-  
1076 variation with biogeography than previously thought. More studies with larger samples,  
1077 when available, are necessary to determine if this structuring is driven by a phylogenetic  
1078 or palaeolatitudinal factor, or a combination of both.

## 1079 **ACKNOWLEDGEMENTS**

1080 We thank C. Griffin and A. Jones for sharing unpublished photographs that  
1081 allowed the estimation of the femoral length of some specimens; S. Spiekman for  
1082 discussion about measurements in some early archosauromorphs; and O. Lehmann for  
1083 helping to resolve doubts about the R language. We appreciate the help of multiple  
1084 curator and collection managers that allowed us to study Permian to Early Jurassic  
1085 archosauromorph specimens in South and North America, Africa, Europe, Asia and  
1086 Australia. We thank the reviewers Pedro Godoy and Roland Sookias, the Associate  
1087 Editor Max Langer, and other editors of *Ameghiniana*, for their comments, which  
1088 improved the quality of the final version of the manuscript. This research was funded by  
1089 the Agencia Nacional de Promoción Científica y Técnica (PICT 2018–01186 to MDE).  
1090 This is J.M.L.’s R-384 contribution to the Instituto de Estudios Andinos Don Pablo  
1091 Groeber.

## 1092 **REFERENCES**

1093 Agnolin, F. L., & Rozadilla, S. (2017). Phylogenetic reassessment of *Pisanosaurus*  
1094 *mertii*, Casamiquela, 1967, a basal dinosauriform from the Late Triassic of  
1095 Argentina. *Journal of Systematic Palaeontology*, 16(10), 853–879.

- 1096 Allen, B. J., Stubbs, T. L., Benton, M. J., & Puttick, M. N. (2019). Archosauromorph  
1097 extinction selectivity during the Triassic–Jurassic mass  
1098 extinction. *Palaeontology*, 62(2), 211–224.
- 1099 Anderson, J. F., Hall-Martin, A. & Russell, D. A. (1985). Long bone circumference and  
1100 weight in mammals, birds and dinosaurs. *Journal of Zoology*, 207, 53–61.
- 1101 Bakker, R. T. (1977). Tetrapod mass extinctions—a model of the regulation of  
1102 speciation rates and immigration by cycles of topographic diversity. In  
1103 *Developments in Palaeontology and Stratigraphy* (Vol. 5, pp. 439–468).  
1104 Elsevier Scientific Publishing, Amsterdam.
- 1105 Bapst, D. W. (2012). paleotree: an R package for paleontological and phylogenetic  
1106 analyses of evolution. *Methods in Ecology and Evolution*, 3(5), 803–807.
- 1107 Baron, M. G., Norman, D. B., & Barrett, P. M. (2017). A new hypothesis of dinosaur  
1108 relationships and early dinosaur evolution. *Nature*, 543(7646), 501–506.
- 1109 Barrett, P. M., Nesbitt, S. J., & Peecook, B. R. (2015). A large-bodied silesaurid from  
1110 the Lifua Member of the Manda beds (Middle Triassic) of Tanzania and its  
1111 implications for body-size evolution in Dinosauromorpha. *Gondwana Research*,  
1112 27(3), 925–931.
- 1113 Blakey, R. (2006). Mollweide plate tectonic maps  
1114 <http://jan.ucc.nau.edu/~rcb7/mollglobe.html>, February 2020.
- 1115 Benton, M. J. (1979). Ectothermy and the success of dinosaurs. *Evolution*, 983–997.
- 1116 Benton, M. J. (1983). Dinosaur success in the Triassic: a noncompetitive ecological  
1117 model. *The Quarterly Review of Biology*, 58(1), 29–55.
- 1118 Benson, R. B. (2018). Dinosaur macroevolution and macroecology. *Anual Review of  
1119 Ecology, Evolution, and Systematics*, 49, 379–408.
- 1120 Benson, R. B., Godoy, P. L., Bronzati, M., Butler, R., & Gearty, W. (2021).  
1121 Reconstructed evolutionary patterns for crocodile-line archosaurs demonstrate  
1122 impact of failure to log-transform body size data. doi:10.31233/osf.io/k3dwf
- 1123 Bergmann, C. (1847). Über die Verhältnisse der Wärmeökonomie der Thiere zu ihrer  
1124 Grösse. *Göttinger Studien*, 3(1), 595–708.
- 1125 Bernardi, M., Klein, H., Petti, F. M., & Ezcurra, M. D. (2015). The origin and early  
1126 radiation of archosauriforms: integrating the skeletal and footprint record. *PLoS  
1127 One*, 10(6), e0128449.
- 1128 Beyl, A., Nesbitt, S., & Stocker, M. R. (2020). An Otischalkian dinosauromorph  
1129 assemblage from the Los Esteros Member (Santa Rosa Formation) of New

- 1130 Mexico and its implications for biochronology and lagerpetid body size. *Journal*  
1131 *of Vertebrate Paleontology*, 40(1), e1765788.
- 1132 Brusatte, S. L., Benton, M. J., Ruta, M., & Lloyd, G. T. (2008a). Superiority,  
1133 competition and opportunism in the evolutionary radiation of dinosaurs. *Science*,  
1134 321(5895), 1485–1488.
- 1135 Brusatte, S. L., Benton, M. J., Ruta, M., & Lloyd, G. T. (2008b). The first 50 Myr of  
1136 dinosaur evolution: macroevolutionary pattern and morphological disparity.  
1137 *Biology Letters*, 4(6), 733–736.
- 1138 Butler, R. J., Barrett, P. M., Abel, R. L., & Gower, D. J. (2009). A possible  
1139 ctenosauriscid archosaur from the Middle Triassic Manda Beds of Tanzania.  
1140 *Journal of Vertebrate Paleontology*, 29(4), 1022–1031.
- 1141 Butler, R. J., Nesbitt, S. J., Charig, A. J., Gower, D. J., & Barrett, P. M. (2017).  
1142 *Mandasuchus tanyauchen*, gen. et sp. nov., a pseudosuchian archosaur from the  
1143 Manda Beds (? Middle Triassic) of Tanzania. *Journal of Vertebrate*  
1144 *Paleontology*, 37(1), 96–121.
- 1145 Button, D. J., Lloyd, G. T., Ezcurra, M. D., & Butler, R. J. (2017). Mass extinctions  
1146 drove increased global faunal cosmopolitanism on the supercontinent  
1147 Pangaea. *Nature Communications*, 8(1), 1–8.
- 1148 Campione, N. E., & Evans, D. C. (2012). A universal scaling relationship between body  
1149 mass and proximal limb bone dimensions in quadrupedal terrestrial tetrapods.  
1150 *BMC Biology*, 10(1), 1–22.
- 1151 Campione, N. E., & Evans, D. C. (2020). The accuracy and precision of body mass  
1152 estimation in non - avian dinosaurs. *Biological Reviews*, 95(6), 1759–1797.
- 1153 Chen, Z. Q., & Benton, M. J. (2012). The timing and pattern of biotic recovery  
1154 following the end-Permian mass extinction. *Nature Geoscience*, 5(6), 375–383.
- 1155 Clements, J.F. (2007). *The Clements checklist of birds of the world, 6th edition*. Cornell  
1156 University Press, Ithaca.
- 1157 Cope, E. D. (1887). Zittel's manual of palaeontology. *American Naturalist*, 21(11),  
1158 1014–1019.
- 1159 Cubo, J., & Jalil, N. E. (2019). Bone histology of *Azendohsaurus laaroussii*:  
1160 Implications for the evolution of thermometabolism in  
1161 Archosauromorphia. *Paleobiology*, 45(2), 317–330.
- 1162 Desojo, J. B., Baczkó, von M. B., & Rauhut, O. W. M. (2020a). Anatomy, taxonomy  
1163 and phylogenetic relationships of *Prestosuchus chiniquensis* (Archosauria:

- 1164 Pseudosuchia) from the original collection of von Huene, Middle–Late Triassic  
1165 of southern Brazil. *Paleontologia Electronica*, 23, a04.
- 1166 Desojo, J. B., Fiorelli, L. E., Ezcurra, M. D., Martinelli, A. G., Ramezani, J., Da Rosa,  
1167 Á. A., Baczkó, von M. B., Trottéyn, M. J., Montefeltro, F. C., Ezpeleta, M., &  
1168 Langer, M. C. (2020b). The Late Triassic Ischigualasto Formation at Cerro Las  
1169 Lajas (La Rioja, Argentina): fossil tetrapods, high-resolution chronostratigraphy,  
1170 and faunal correlations. *Scientific reports*, 10(1), 1–34.
- 1171 Dilkes, D. W., & Arcucci, A. (2012). *Proterochamps barrionuevoi* (Archosauriformes:  
1172 Proterochampsia) from the Late Triassic (Carnian) of Argentina and a  
1173 phylogenetic analysis of Proterochampsia. *Palaeontology*, 5, 853–885.
- 1174 Dunne, E. M., Farnsworth, A., Greene, S. E., Lunt, D. J., & Butler, R. J. (2020).  
1175 Climatic drivers of latitudinal variation in Late Triassic tetrapod  
1176 diversity. *Palaeontology*, 64(1), 101–117.
- 1177 Ezcurra, M. D. (2010a). Biogeography of Triassic tetrapods: evidence for provincialism  
1178 and driven sympatric cladogenesis in the early evolution of modern tetrapod  
1179 lineages. *Proceedings of the Royal Society B: Biological Sciences*, 277(1693),  
1180 2547–2552.
- 1181 Ezcurra, M. D. (2010b). A new early dinosaur (Saurischia: Sauropodomorpha) from the  
1182 Late Triassic of Argentina: a reassessment of dinosaur origin and  
1183 phylogeny. *Journal of Systematic Palaeontology*, 8(3), 371–425.
- 1184 Ezcurra, M. D. (2016). The phylogenetic relationships of basal archosauromorphs, with  
1185 an emphasis on the systematic of proterosuchian archosauriforms. *PeerJ*, 4,  
1186 e1778.
- 1187 Ezcurra, M. D., & Butler, R. J. (2018). The rise of the ruling reptiles and ecosystem  
1188 recovery from the Permo–Triassic mass extinction. *Proceedings of the Royal  
1189 Society B*, 285(1880), 20180361.
- 1190 Ezcurra, M. D., Butler, R. J., Maidment, S. C., Sansom, I. J., Meade, L. E., & Radley, J.  
1191 D. (2021a). A revision of the early neotheropod genus *Sarcosaurus* from the  
1192 Early Jurassic (Hettangian–Sinemurian) of central England. *Zoological Journal  
1193 of the Linnean Society*, 191(1), 113–149.
- 1194 Ezcurra, M. D., Fiorelli, L. E., Martinelli, A. G., Rocher, S., Baczkó, von M. B.,  
1195 Ezpeleta, M., Taborda, J. R. A., Hechenleitner, E. M., Trottéyn, M. J., & Desojo,  
1196 J. B. (2017). Deep faunistic turnovers preceded the rise of dinosaurs in  
1197 southwestern Pangaea. *Nature Ecology & Evolution*, 1(10), 1477–1483.

- 1198 Ezcurra, M. D., Fiorelli, L. E., Trottay, M. J., Martinelli, A. G., & Desojo, J. B.  
1199 (2020a). The rhynchosaur record, including a new stenaulorhynchine taxon,  
1200 from the Chañares Formation (upper Ladinian–? lowermost Carnian levels) of  
1201 La Rioja Province, north-western Argentina. *Journal of Systematic*  
1202 *Palaeontology*, 18(23), 1907–1938.
- 1203 Ezcurra, M. D., Gentil, A. R., Jones, A., & Butler, R. J. (2021b). Early  
1204 archosauromorphs: the crocodile and dinosaur precursors. In: Alderton, D, &  
1205 Elias, S. A. (eds). *Encyclopedia of Geology, Second Edition* (pp. 175–185).  
1206 Elsevier Scientific Publishing, Amsterdam.
- 1207 Ezcurra, M. D., Montefeltro, F. C., & Butler, R. J. (2016). The early evolution of  
1208 rhynchosauroids. *Frontiers in Ecology and Evolution*, 3, 142.
- 1209 Ezcurra, M. D., Montefeltro, F. C., Pinheiro, F. L., Trottay, M. J., Gentil, A. R.,  
1210 Lehmann, O. E., & Pradelli, L. A. (2021c). The stem-archosaur evolutionary  
1211 radiation in South America. *Journal of South American Earth Sciences*, 105,  
1212 102935.
- 1213 Ezcurra, M. D., Nesbitt, S. J., Bronzati, M., Dalla Vecchia, F. M., Agnolin, F. L.,  
1214 Benson, R. B., Brissón, E. F., Cabreira, S. F., Evers, S. W., Gentil, A. R., Irmis,  
1215 R. B., Martinelli, A. G., Novas, F. E., Roberto-Da-Silva, Smith, N. D., Stocker,  
1216 M. R., Turner, A. H., & Langer, M. C. (2020b). Enigmatic dinosaur precursors  
1217 bridge the gap to the origin of Pterosauria. *Nature*, 588, 445–449.
- 1218 Ezcurra, M. D., Scheyer, T. M., & Butler, R. J. (2014). The origin and early evolution  
1219 of Sauria: reassessing the Permian saurian fossil record and the timing of the  
1220 crocodile–lizard divergence. *PLoS One*, 9(2), e89165.
- 1221 Ezcurra, M. D., Velozo, P., Meneghel, M., & Piñeiro, G. (2015). Early  
1222 archosauromorph remains from the Permo-Triassic Buena Vista Formation of  
1223 north-eastern Uruguay. *PeerJ*, 3, e776.
- 1224 Feduccia, A. (1995). Explosive evolution in Tertiary birds and mammals. *Science*, 267,  
1225 637–638.
- 1226 Fernandez, B. M. V., Ezcurra, M. D., & Bona, P. (2020). New embryological and  
1227 palaeontological evidence sheds light on the evolution of the archosauromorph  
1228 ankle. *Scientific Reports*, 10(1), 5150.
- 1229 Foth, C., Ezcurra, M. D., Sookias, R. B., Brusatte, S. L., & Butler, R. J. (2016).  
1230 Unappreciated diversification of stem archosaurs during the Middle Triassic  
1231 predated the dominance of dinosaurs. *BMC Evolutionary Biology*, 16(1), 188.

- 1232 Franceschi, M., Dal Corso, J., Posenato, R., Roghi, G., Masetti, D., & Jenkyns, H. C.  
1233 (2014). Early Pliensbachian (Early Jurassic) C-isotope perturbation and the  
1234 diffusion of the Lithiotis Fauna: insights from the western  
1235 Tethys. *Palaeogeography, Palaeoclimatology, Palaeoecology*, 410, 255–263.
- 1236 Gauthier, J., Kluge, A. G. & Rowe, T. (1988). Amniote phylogeny and the importance  
1237 of fossils. *Cladistics*, 4, 105–209.
- 1238 Godoy, P. L., Benson, R. B., Bronzati, M., & Butler, R. J. (2019). The multi-peak  
1239 adaptive landscape of crocodylomorph body size evolution. *BMC Evolutionary  
1240 Biology*, 19(1), 167.
- 1241 Goloboff, P. A., & Pol, D. (2002). Semi - strict supertrees. *Cladistics*, 18(5), 514–525.
- 1242 Grady, J. M., Enquist, B. J., Dettweiler-Robinson, E., Wright, N. A., & Smith, F. A.  
1243 (2014). Evidence for mesothermy in dinosaurs. *Science*, 344(6189), 1268–1272.
- 1244 Grauvogel-Stamm, L., & Ash, S. R. (2005). Recovery of the Triassic land flora from  
1245 the end-Permian life crisis. *Comptes Rendus Palevol*, 4(6–7), 593–608.
- 1246 Grellet-Tinner, G. (2006). Oology and the evolution of thermophysiology in saurischian  
1247 dinosaurs: homeotherm and endotherm deinonychosaurians? *Papéis Avulsos de  
1248 Zoologia*, 46(1), 1–10.
- 1249 Grinham, L. R., VanBuren, C. S., & Norman, D. B. (2019). Testing for a facultative  
1250 locomotor mode in the acquisition of archosaur bipedality. *Royal Society Open  
1251 Science*, 6(7), 190569.
- 1252 Guillerme, T., Puttik, M. N., Marcy, A. E., & Weisbecker, V. (2020). Shifting spaces:  
1253 which disparity or dissimilarity metrics best summarise occupancy in  
1254 multidimensional spaces? *Ecology and Evolution*, 10(14), 7261–7275.
- 1255 Hammer, Ø., Harper, D. A., & Ryan, P. D. (2001). PAST: Paleontological statistics  
1256 software package for education and data analysis. *Palaeontologia  
1257 electronica*, 4(1), 9.
- 1258 Head, J. J., Bloch, J. I., Hastings, A. K., Bourque, J. R., Cadena, E. A., Herrera, F. A.,  
1259 Polly, P., & Jaramillo, C. A. (2009). Giant boid snake from the Palaeocene  
1260 neotropics reveals hotter past equatorial temperatures. *Nature*, 457(7230), 715–  
1261 717.
- 1262 Hesselbo, S. P., Robinson, S. A., Surlyk, F., & Piasecki, S. (2002). Terrestrial and  
1263 marine extinction at the Triassic–Jurassic boundary synchronized with major  
1264 carbon–cycle perturbation: A link to initiation of massive  
1265 volcanism? *Geology*, 30(3), 251–254.

- 1266 Irmis, R. B. (2011). Evaluating hypotheses for the early diversification of dinosaurs.  
1267         *Earth Environmental Science Transactions of the Royal Society of Edinburgh*  
1268         *101*(3–4), 397–426.
- 1269 Irmis, R. B., Mundil, R., Martz, J. W., & Parker, W. G. (2011). High–resolution U–Pb  
1270         ages from the Upper Triassic Chinle Formation (New Mexico, USA) support a  
1271         diachronous rise of dinosaurs. *Earth and Planetary Science Letters*, *309*(3–4),  
1272         258–267.
- 1273 Irmis, R. B., & Whiteside, J. H. (2012). Delayed recovery of non–marine tetrapods after  
1274         the end–Permian mass extinction tracks global carbon cycle. *Proceedings of the*  
1275         *Royal Society B: Biological Sciences*, *279*(1732), 1310–1318.
- 1276 Jones, A. S., & Butler, R. J. (2018). A new phylogenetic analysis of Phytosauria  
1277         (Archosauria: Pseudosuchia) with the application of continuous and geometric  
1278         morphometric character coding. *PeerJ*, *6*, e5901.
- 1279 Langer, M. C., Bittencourt, J. S., & Schultz, C. L. (2011). A reassessment of the basal  
1280         dinosaur *Guaibasaurus candelariensis*, from the Late Triassic Caturrita  
1281         Formation of south Brazil. *Earth and Environmental Science Transactions of the*  
1282         *Royal Society of Edinburgh*, *101*(3–4), 301–332.
- 1283 Langer, M. C., Da Rosa, Á. A., & Montefeltro, F. C. (2017). *Supradapedon* revisited:  
1284         geological explorations in the Triassic of southern Tanzania. *PeerJ*, *5*, e4038.
- 1285 Langer, M. C., Ramezani, J., & Da Rosa, Á. A. (2018). U–Pb age constraints on  
1286         dinosaur rise from south Brazil. *Gondwana Research*, *57*, 133–140.
- 1287 Leardi, J. M., Pol, D. & Clark, J. M. (2017). Detailed anatomy of the braincase  
1288         of *Macelognathus vagans* Marsh, 1884 (Archosauria, Crocodylomorpha) using  
1289         high resolution tomography and new insights on basal crocodylomorph  
1290         phylogeny. *PeerJ*, *5*, e2801.
- 1291 Liu, J., Li, L., & Li, X. W. (2013). SHRIMP U–Pb zircon dating of the Triassic  
1292         Ermaying and Tongchuan formations in Shanxi, China and its stratigraphic  
1293         implications. *Vertebrata Pal Asiatica*, *51*, 162–168.
- 1294 Looy, C. V., Brugman, W. A., Dilcher, D. L., & Visscher, H. (1999). The delayed  
1295         resurgence of equatorial forests after the Permian–Triassic ecologic  
1296         crisis. *Proceedings of the national Academy of Sciences*, *96*(24), 13857–13862.
- 1297 Maddison, W. P., & D. R. Maddison. (2019). Mesquite: a modular system for  
1298         evolutionary analysis. Version 3.61 <http://www.mesquiteproject.org>

- 1299 Makarieva, A. M., Gorshkov, V. G., & Li, B. L. (2005). Gigantism, temperature and  
1300 metabolic rate in terrestrial poikilotherms. *Proceedings of the Royal Society B: Biological Sciences*, 272(1578), 2325–2328.
- 1301
- 1302 Marsicano, C. A., Irmis, R. B., Mancuso, A. C., Mundil, R., & Chemale, F. (2016). The  
1303 precise temporal calibration of dinosaur origins. *Proceedings of the National  
1304 Academy of Sciences* 113(3), 509–513.
- 1305 Martinelli, A.G., Francischini, H., Dentzien-Dias, P.C., Soares, M.B., & Schultz, C.L.  
1306 (2017). The oldest archosauromorph from South America: postcranial remains  
1307 from the Guadalupian (mid-Permian) Rio do Rasto Formation (Paraná basin),  
1308 southern Brazil. *Historical Biology*, 29(1), 76–84.
- 1309 Martínez, R. N., Sereno, P. C., Alcober, O. A., Colombi, C. E., Renne, P. R., Montañez,  
1310 I. P., & Currie, B. S. (2011). A basal dinosaur from the dawn of the dinosaur era  
1311 in southwestern Pangaea. *Science*, 331(6014), 206–210.
- 1312 McPhee, B. W., Bordy, E. M., Sciscio, L., & Choiniere, J. N. (2017). The  
1313 sauropodomorph biostratigraphy of the Elliot Formation of southern Africa:  
1314 tracking the evolution of Sauropodomorpha across the Triassic–Jurassic  
1315 boundary. *Acta Paleontologica Polonica*, 62(3), 441–465.
- 1316 Nesbitt, S. J. (2011). The early evolution of archosaurs: relationships and the origin of  
1317 major clades. *Bulletin of the American Museum of Natural History*, 2011(352),  
1318 1–292.
- 1319 Nesbitt, S. J., Desojo, J. B. & Irmis, R. B. (2013). Anatomy, phylogeny and  
1320 palaeobiology of early archosaurs and their kin. *Geological Society of London, Special Publications*, 379(1), 1–7.
- 1321
- 1322 Nesbitt, S. J., Flynn, J. J., Pritchard, A. C., Parrish, J. M., Ranivoharimanana, L., &  
1323 Wyss, A. R. (2015). Postcranial osteology of *Azendohsaurus madagaskarensis*  
1324 (? Middle to Upper Triassic, Isalo Group, Madagascar) and its systematic  
1325 position among stem archosaur reptiles. *Bulletin of the American Museum of  
1326 Natural History*, 2015(398), 1–126.
- 1327 Nesbitt, S. J., Langer, M. C., & Ezcurra, M. D. (2020). The anatomy of *Asilisaurus  
1328 kongwe*, a dinosauriform from the Lifua Member of the Manda Beds (~ Middle  
1329 Triassic) of Africa. *The Anatomical Record*, 303(4), 813–873.
- 1330 Nesbitt, S. J., & Norell, M. A. (2006). Extreme convergence in the body plans of an  
1331 early suchian (Archosauria) and ornithomimid dinosaurs (Theropoda).  
1332 *Proceedings of the Royal Society B: Biological Sciences*, 273(1590), 1045–1048.

- 1333 Nesbitt, S. J., Stocker, M. R., Chatterjee, S., Horner, J. R., & Goodwin, M. B. (2021). A  
1334 remarkable group of thick - headed Triassic Period archosauromorphs with a  
1335 wide, possibly Pangean distribution. *Journal of Anatomy*. doi:  
1336 10.1111/joa.13414
- 1337 Nesbitt, S. J., Stocker, M. R., Parker, W. G., Wood, T. A., Sidor, C. A., & Angielczyk,  
1338 K. D. (2017). The braincase and endocast of *Parringtonia gracilis*, a Middle  
1339 Triassic suchian (Archosaur: Pseudosuchia). *Journal of Vertebrate  
1340 Paleontology*, 37(1), 122–141.
- 1341 O'Connor, P. M. (2006). Postcranial pneumaticity: an evaluation of soft - tissue  
1342 influences on the postcranial skeleton and the reconstruction of pulmonary  
1343 anatomy in archosaurs. *Journal of morphology*, 267(10), 1199–1226.
- 1344 Olsen, P. E., Kent, D. V., Sues, H. D., Koeberl, C., Huber, H., Montanari, A., Rainforth,  
1345 E. C., Forwell, S. J., Szajna, B., & Hartline, B. W. (2002). Ascent of dinosaurs  
1346 linked to an iridium anomaly at the Triassic–Jurassic  
1347 boundary. *Science*, 296(5571), 1305–1307.
- 1348 Otero, A., Krupandan, E., Pol, D., Chinsamy, A., & Choiniere, J. (2015). A new basal  
1349 sauropodiform from South Africa and the phylogenetic relationships of basal  
1350 sauropodomorphs. *Zoological Journal of the Linnean Society*, 174(3), 589–634.
- 1351 Ottone, E. G., Monti, M., Marsicano, C. A., Marcelo, S., Naipauer, M., Armstrong, R.,  
1352 & Mancuso, A. C. (2014). A new Late Triassic age for the Puesto Viejo Group  
1353 (San Rafael depocenter, Argentina): SHRIMP U–Pb zircon dating and  
1354 biostratigraphic correlations across southern Gondwana. *Journal of South  
1355 American Earth Sciences*, 56, 186–199.
- 1356 Park, O. (1949). Application of the converse Bergmann principle to the carabid beetle,  
1357 *Dicaelus purpuratus*. *Physiological Zoology*, 22(4), 359–372.
- 1358 Parker, W. G. (2016). Revised phylogenetic analysis of the Aetosauria (Archosauria:  
1359 Pseudosuchia); assessing the effects of incongruent morphological character  
1360 sets. *PeerJ*, 4, e1583.
- 1361 Payne, J. L., Lehrmann, D. J., Wei, J., Orchard, M. J., Schrag, D. P., & Knoll, A. H.  
1362 (2004). Large perturbations of the carbon cycle during recovery from the end–  
1363 Permian extinction. *Science*, 305(5683), 506–509.

- 1364 Pinheiro, J., Bates, D., DebRoy, S., Sarkar, D., & Team, R. C. (2020). nlme: Linear and  
1365 Nonlinear Mixed Effects Models: R package version 3.1–148, [https://CRAN.R-  
1366 project.org/package=nlme](https://CRAN.R-project.org/package=nlme)
- 1367 Ramezani, R., Fastovsky, D. E., & Bowring, S. A. (2014). Revised chronostratigraphy  
1368 of the lower Chinle Formation strata in Arizona and New Mexico (USA): high-  
1369 precision U–Pb geochronological constraints on the Late Triassic evolution of  
1370 dinosaurs. *American Journal of Science*, 314(6), 981–1008.
- 1371 Ramezani, J., Hoke G. D., Fastovsky D. E., Bowring S. A., Therrien F., Dworkin S. I.,  
1372 Atchley S. C., & Nordt L. C. (2011). High-precision U–Pb zircon  
1373 geochronology of the Late Triassic Chinle Formation, Petrified Forest National  
1374 Park (Arizona, USA): temporal constraints on the early evolution of dinosaurs.  
1375 *Geological Society of America Bulletin*, 123(11–12), 2142–2159.
- 1376 Raup, D. M. (1977). Probabilistic models in evolutionary paleobiology: A random walk  
1377 through the fossil record produces some surprising results. *American  
1378 Scientist*, 65(1), 50–57.
- 1379 Raup, D. M., & Sepkoski, J. J. (1982). Mass extinctions in the marine fossil  
1380 record. *Science*, 215(4539), 1501–1503.
- 1381 Revell, L. J. (2012). phytools: an R package for phylogenetic comparative biology (and  
1382 other things). *Methods in ecology and evolution*, 3(2), 217–223.
- 1383 Rodrigues, J. F. M., Olalla - Tárraga, M. Á., Iverson, J. B., & Diniz - Filho, J. A. F.  
1384 (2018). Temperature is the main correlate of the global biogeography of turtle  
1385 body size. *Global Ecology and Biogeography*, 27(4), 429–438.
- 1386 Rubidge, B. S., Erwin, D. H., Ramezani, J., Bowring, S. A., & de Klerk, W. J. (2013).  
1387 High-precision temporal calibration of Late Permian vertebrate biostratigraphy:  
1388 U–Pb zircon constraints from the Karoo Supergroup, South  
1389 Africa. *Geology*, 41(3), 363–366.
- 1390 Sengupta, S., Ezcurra, M. D., & Bandyopadhyay, S. (2017). A new horned and long-  
1391 necked herbivorous stem–archosaur from the Middle Triassic of India. *Scientific  
1392 reports*, 7(1), 1–9.
- 1393 Seymour, R. S., Bennett-Stamper, C. L., Johnston, S. D., Carrier, D. R., & Grigg, G. C.  
1394 (2004). Evidence for endothermic ancestors of crocodiles at the stem of  
1395 archosaur evolution. *Physiological and Biochemical Zoology*, 77(6), 1051–1067.
- 1396 Simpson, G. G. (1944). *Tempo and Mode in Evolution* (No. 15). Columbia University  
1397 Press, New York.

- 1398 Sookias, R. B. (2016). The relationships of the Euparkeriidae and the rise of  
1399 Archosauria. *Royal Society Open Science*, 3(3), 150674.
- 1400 Sookias, R. B., Benson, R. B. J., & Butler, R. J. (2012a). Biology, not environment,  
1401 drives major patterns in maximum tetrapod body size through time. *Biology  
1402 Letters*, 8(4), 674–677.
- 1403 Sookias, R. B., Butler, R. J., & Benson, R. B. (2012b). Rise of dinosaurs reveals major  
1404 body-size transitions are driven by passive processes of trait evolution.  
1405 *Proceedings of the Royal Society of London B*, 279(1736), 2180–2187.
- 1406 Stockdale, M. T., & Benton, M. J. (2021). Environmental drivers of body size evolution  
1407 in crocodile-line archosaurs. *Communications biology*, 4(1), 1–11.
- 1408 Stocker, M. R., Nesbitt, S. J., Criswell, K. E., Parker, W. G., Witmer, L. M., Rowe, T.  
1409 B., Ridgely, R. & Brown, M.A. (2016). A dome-headed stem archosaur  
1410 exemplifies convergence among dinosaurs and their distant relatives. *Current  
1411 Biology*, 26(19), 2674–2680.
- 1412 Sun, Y., Joachimski, M. M., Wignall, P. B., Yan, C., Chen, Y., Jiang, H., & Lai, X.  
1413 (2012). Lethally hot temperatures during the Early Triassic  
1414 greenhouse. *Science*, 338(6105), 366–370.
- 1415 Turner, A. H., & Nesbitt, S. J. (2013). Body size evolution during the Triassic  
1416 archosauriform radiation. *Geological Society of London, Special Publications*,  
1417 379(1), 573–597.
- 1418 Wang, J., Wu, C., Li, Z., Zhu, W., Zhou, T., Wu, J., & Wang, J. (2019). Whole - rock  
1419 geochemistry and zircon Hf isotope of Late Carboniferous–Triassic sediments in  
1420 the Bogda region, NW China: Clues for provenance and tectonic  
1421 setting. *Geological Journal*, 54(4), 1853–1877.
- 1422 Whiteside, J. H., & Ward, P. D. (2011). Ammonoid diversity and disparity track  
1423 episodes of chaotic carbon cycling during the early Mesozoic. *Geology*, 39(2),  
1424 99–102.

1425 **FIGURE LEGENDS**

- 1426 **Figure 1.** Time calibrated simplified phylogenetic tree showing the diversity of early  
1427 archosauromorphs between the Permian and Early Jurassic. Phylogenetic relationships  
1428 based on Ezcurra *et al.* (2020a, 2021b). Silhouettes taken from <http://phylopic.org/>  
1429 except: Allokotosauria taken from Sengupta *et al.* (2017); Erpetosuchidae taken and

1430 modified from Nesbitt *et al.* (2017); *Mandasuchus* taken and modified from Butler *et al.*  
1431 (2017); Lagerpetidae taken from Ezcurra *et al.* (2020b); and Silesauridae taken and  
1432 modified from Nesbitt *et al.* (2020).

1433 **Figure 2.** Palaeolatitudinal bins used in the analyses shown on a palaeogeographic  
1434 reconstruction of the Earth during the Early–Middle Triassic. Bin 1 (white), Bin 2  
1435 (orange), Bin 3 (green), Bin 4 (red) and Bin 5 (purple). Image modified from Blakey  
1436 (2006).

1437 **Figure 3.** Body size disparity of Archosauromorpha; **1**, log-transformed femoral length  
1438 through time bins; the mean is indicated with orange diamonds; **2**, standard deviation  
1439 (green); **3**, ranges (purple); and **4**, medians (red) through the nine time bins (alternating  
1440 between grey and white). Significant differences with respect to the previous time  
1441 interval are indicated with an asterisk (\*).

1442 **Figure 4.** Body size disparity of non-archosaurian Archosauromorpha grade  
1443 archosauromorphs; **1**, log-transformed femoral length through time bins; the mean is  
1444 indicated with ~~an~~ orange diamonds; **2**, standard deviation (green); **3**, ranges (purple);  
1445 and **4**, medians (red) through the six time bins (alternating between grey and white).  
1446 Significant differences with respect to the previous time interval are indicated with an  
1447 asterisk (\*).

1448 **Figure 5.** Body size disparity of Pseudosuchia; **1**, log-transformed femoral length  
1449 through time bins; the mean is indicated with orange diamonds; **2**, standard deviation  
1450 (green); **3**, ranges (purple); and **4**, medians (red) through the five time bins (alternating  
1451 between grey and white). Significant differences with respect to the previous time  
1452 interval are indicated with an asterisk (\*).

1453 **Figure 6.** Body size disparity of non-dinosaurian Pan-Aves grade archosauromorphs; **1**,  
1454 log-transformed femoral length through time bins; the mean is indicated with orange

1455 diamonds; **2**, standard deviation (green); **3**, ranges (purple); and **4**, medians (red)  
1456 through the five time bins (alternating between grey and white). Significant differences  
1457 with respect to the previous time interval are indicated with an asterisk (\*).

1458 **Figure 7.** Body size disparity of Sauropodomorpha; **1**, log-transformed femoral length  
1459 through time bins; the mean is indicated with orange diamonds; **2**, standard deviation  
1460 (green); **3**, ranges (purple); and **4**, medians (red) through the four time bins (alternating  
1461 between grey and white). Significant differences with respect to the previous time  
1462 interval are indicated with an asterisk (\*).

1463 **Figure 8.** Body size disparity of Theropoda; **1**, log-transformed femoral length through  
1464 time bins; the mean is indicated with orange diamonds; **2**, standard deviation (green); **3**,  
1465 ranges (purple); and **4**, medians (red) through the four time bins (alternating between  
1466 grey and white). Significant differences with respect to the previous time interval are  
1467 indicated with an asterisk (\*).

1468 **Figure 9.** Body size disparity of Archosauromorpha including species present in more  
1469 than one time bin; **1**, log-transformed femoral length through time bins; the mean is  
1470 indicated with orange diamonds; **2**, standard deviation (green); **3**, ranges (purple); and **4**,  
1471 medians (red) through the nine time bins (alternating between grey and white).  
1472 Significant differences with respect to the previous time interval are indicated with an  
1473 asterisk (\*).

1474 **Figure 10.** Disparity of body size of Archosauromorpha in relation to palaeolatitudinal  
1475 bins; **1**, log-transformed femoral length in relation to palaeolatitudinal bins through the  
1476 Anisian; **2**, medians of the log-transformed femoral length (blue) as a function of the  
1477 palaeolatitudinal bins through the Anisian; **3**, log-transformed femoral length in relation  
1478 to palaeolatitudinal bins through the late Carnian–early Norian; **4**, medians of the log-  
1479 transformed femoral length (blue) as a function of the palaeolatitudinal bins through the

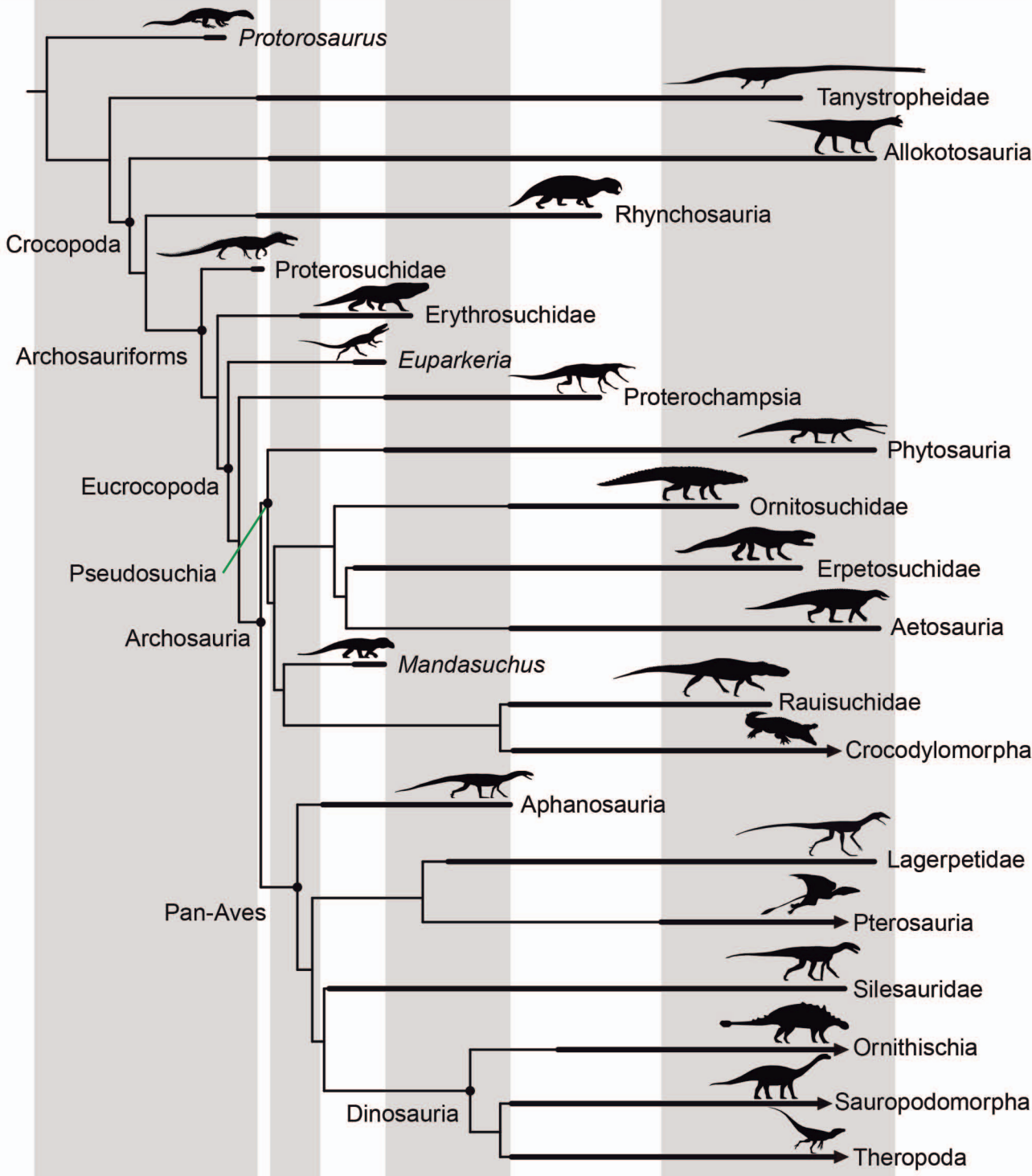
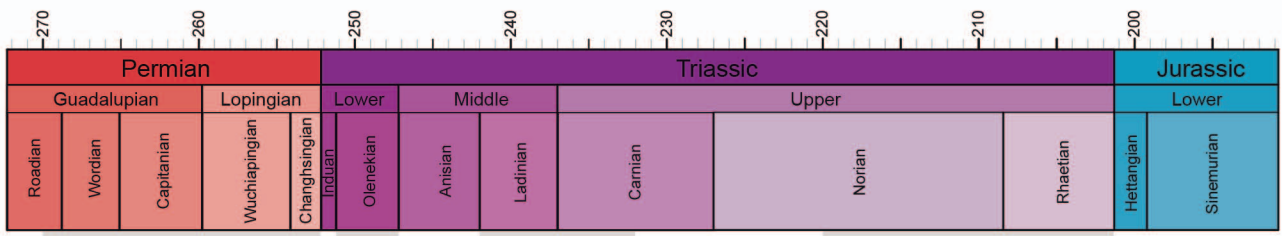
1480 late Carnian–early Norian; **5**, log-transformed femoral length in relation to  
1481 palaeolatitudinal bins through the middle Norian–Rhaetian; and **6**, medians of the log-  
1482 transformed femoral length (blue) as a function of the palaeolatitudinal bins through the  
1483 middle Norian–Rhaetian. The mean is indicated with an orange diamond. Significant  
1484 differences with respect to the previous time interval are indicated with an asterisk (\*).

1485 **Figure 11.** Results of the pGLS regressions plotted on the phylomorphospace generated  
1486 by femoral length and palaeolatitude during the Triassic; **1**, log-transformed femoral  
1487 length in relation to the palaeolatitude for the Anisian archosauromorphs; **2**, for the  
1488 Anisian pseudosuchians; **3**, for the late Carnian–early Norian archosauromorphs; **4**, for  
1489 the late Carnian–early Norian phytosaurs; **5**, for the middle Norian–Rhaetian  
1490 archosauromorphs; and **6**, for the middle Norian–Rhaetian crocodylomorphs. The  
1491 regression for each of the 100 trees is represented by a dotted line. The purple dotted  
1492 lines indicate significant results and the light brown dotted lines indicate non-significant  
1493 results. Each grey point represents a species and the lines joining them represent  
1494 phylogenetic relationships.

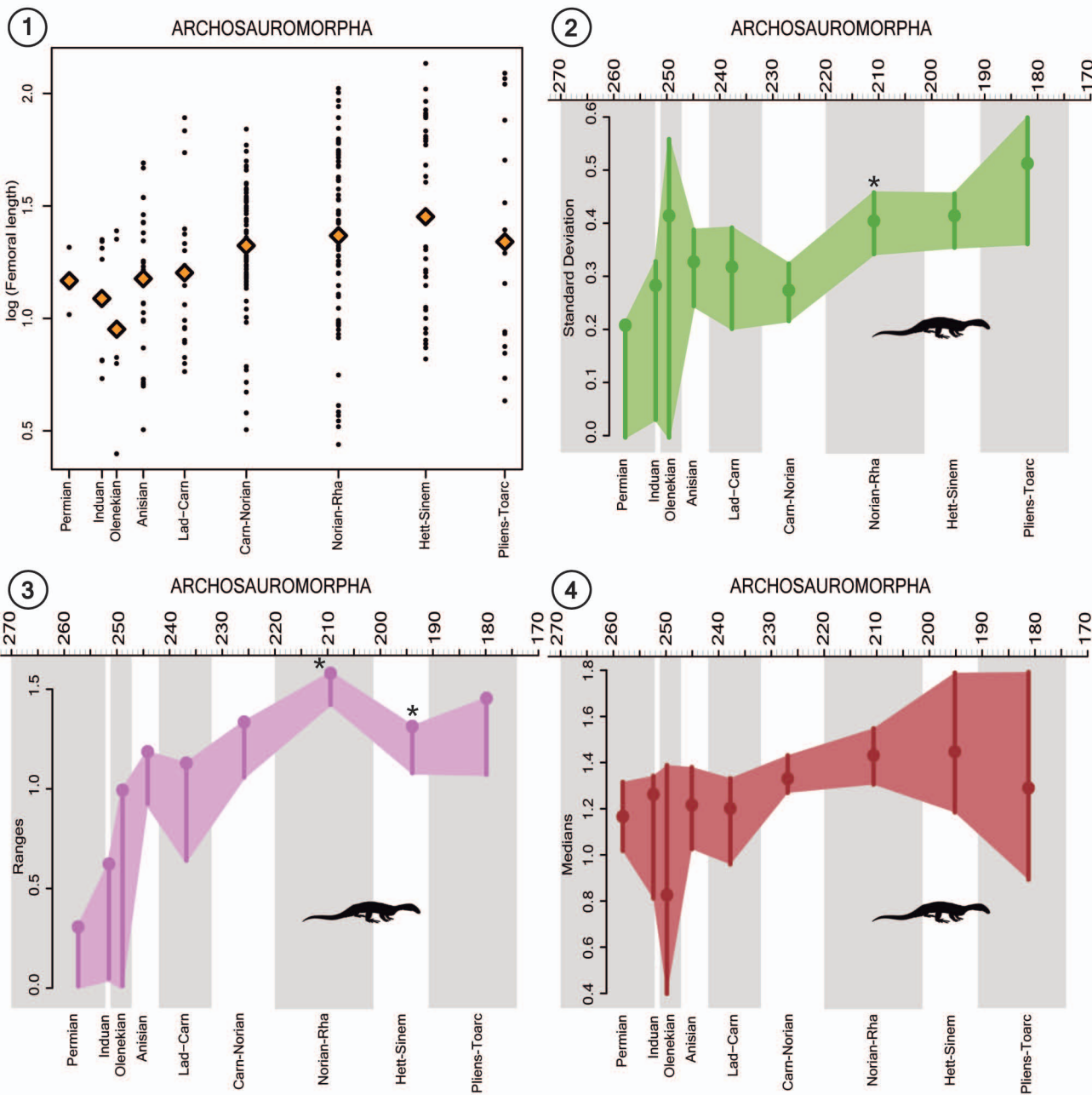
1495 **Figure 12.** Relationship between body size and palaeolatitude through all the Triassic;  
1496 **1**, log-transformed femoral length in relation to the palaeolatitude for crocodylomorphs;  
1497 and **2**, for phytosaurs. The regression for each of the 100 trees is represented by a dotted  
1498 line. The purple dotted lines indicate significant results and the light brown dotted lines  
1499 indicate non-significant results. Each grey point represents a species and the lines  
1500 joining them represent phylogenetic relationships.

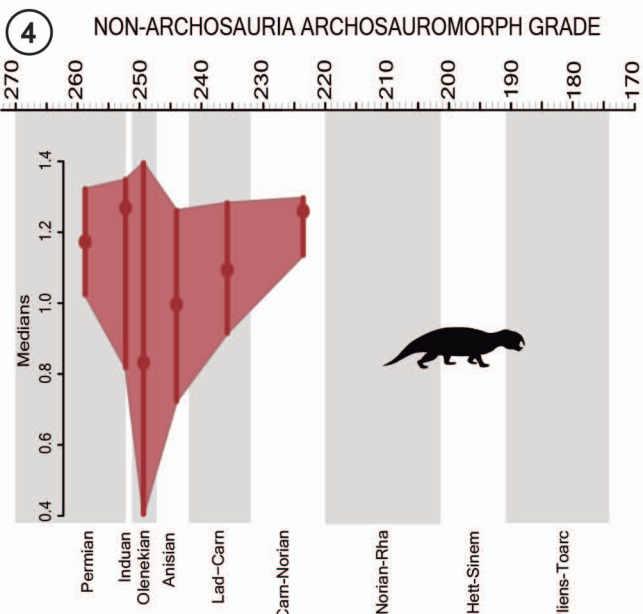
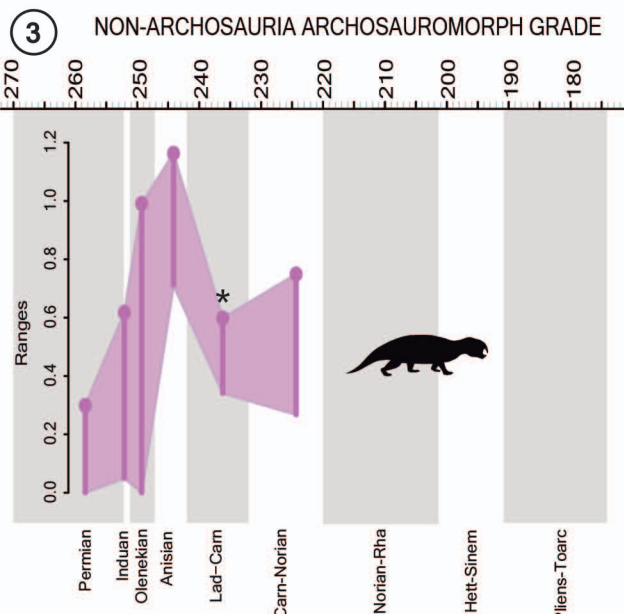
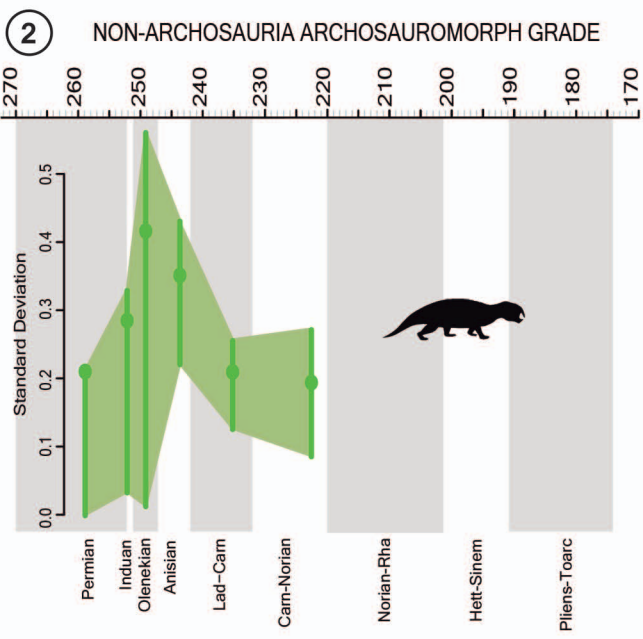
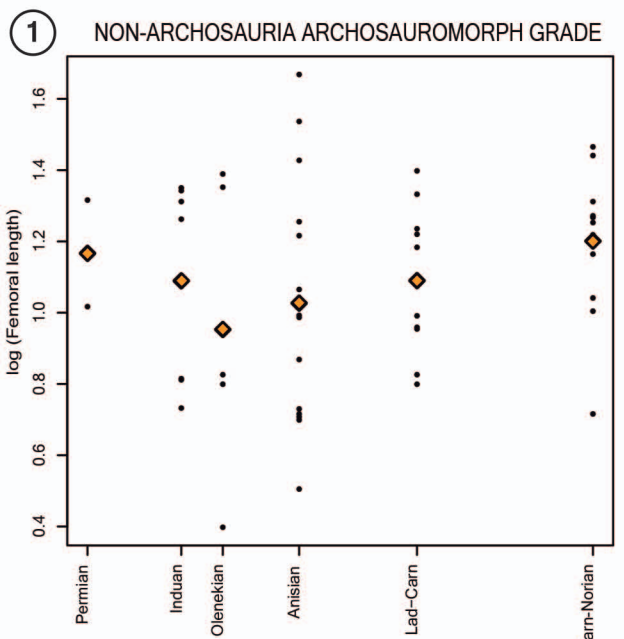
1501 **Figure 13.** Relationship between body size and palaeolatitude through time during the  
1502 Jurassic; **1**, log-transformed femoral length in relation to the palaeolatitude for the late  
1503 Hettangian–Sinemurian archosauromorphs; and **2**, for the late Pliensbachian–Toarcian  
1504 archosauromorphs. The regression for each of the 100 trees is represented by a dotted

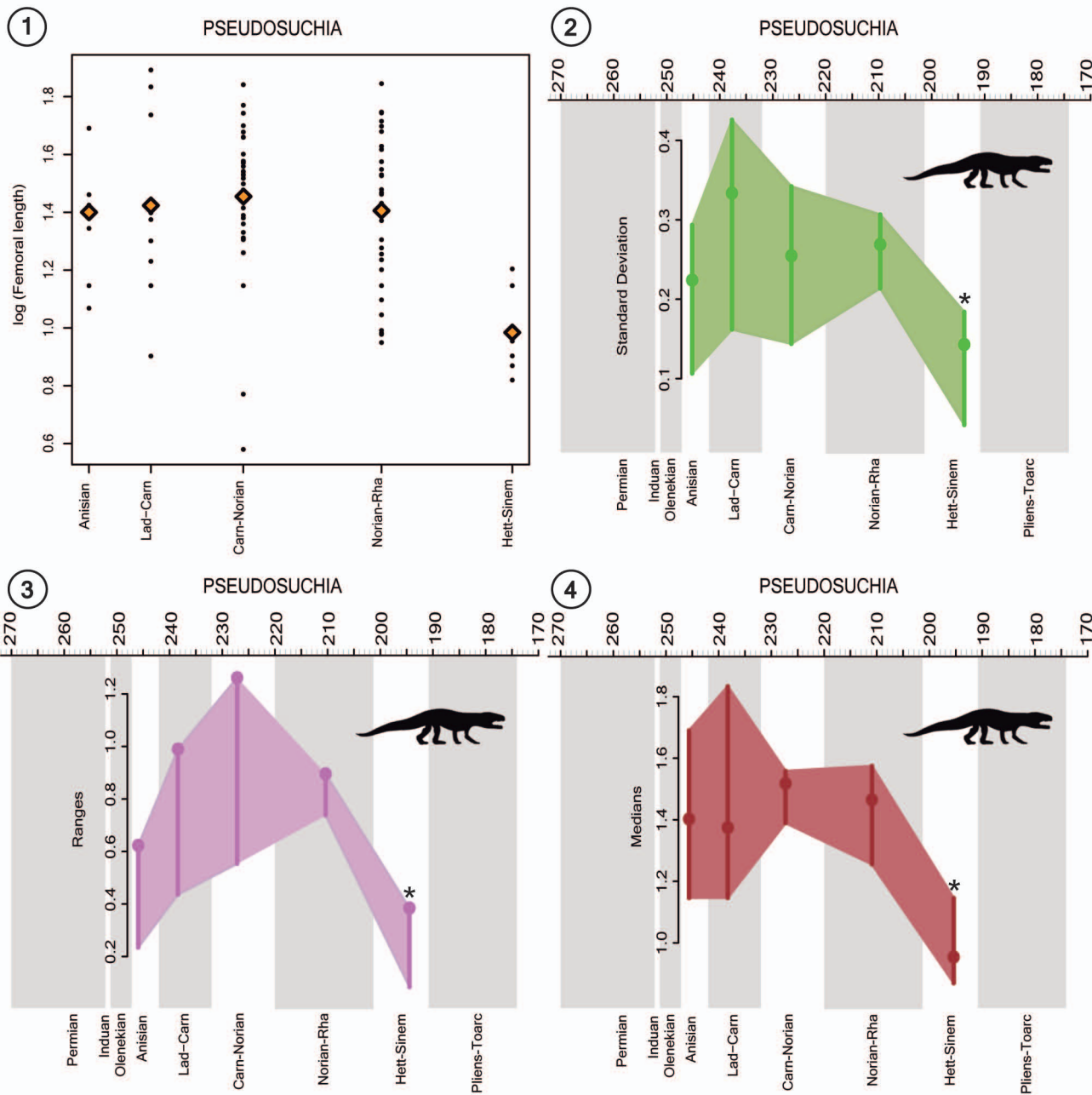
1505 line. The purple dotted lines indicate significant results and the light brown dotted lines  
1506 indicate non-significant results. Each grey point represents a species and the lines  
1507 joining them represent phylogenetic relationships.

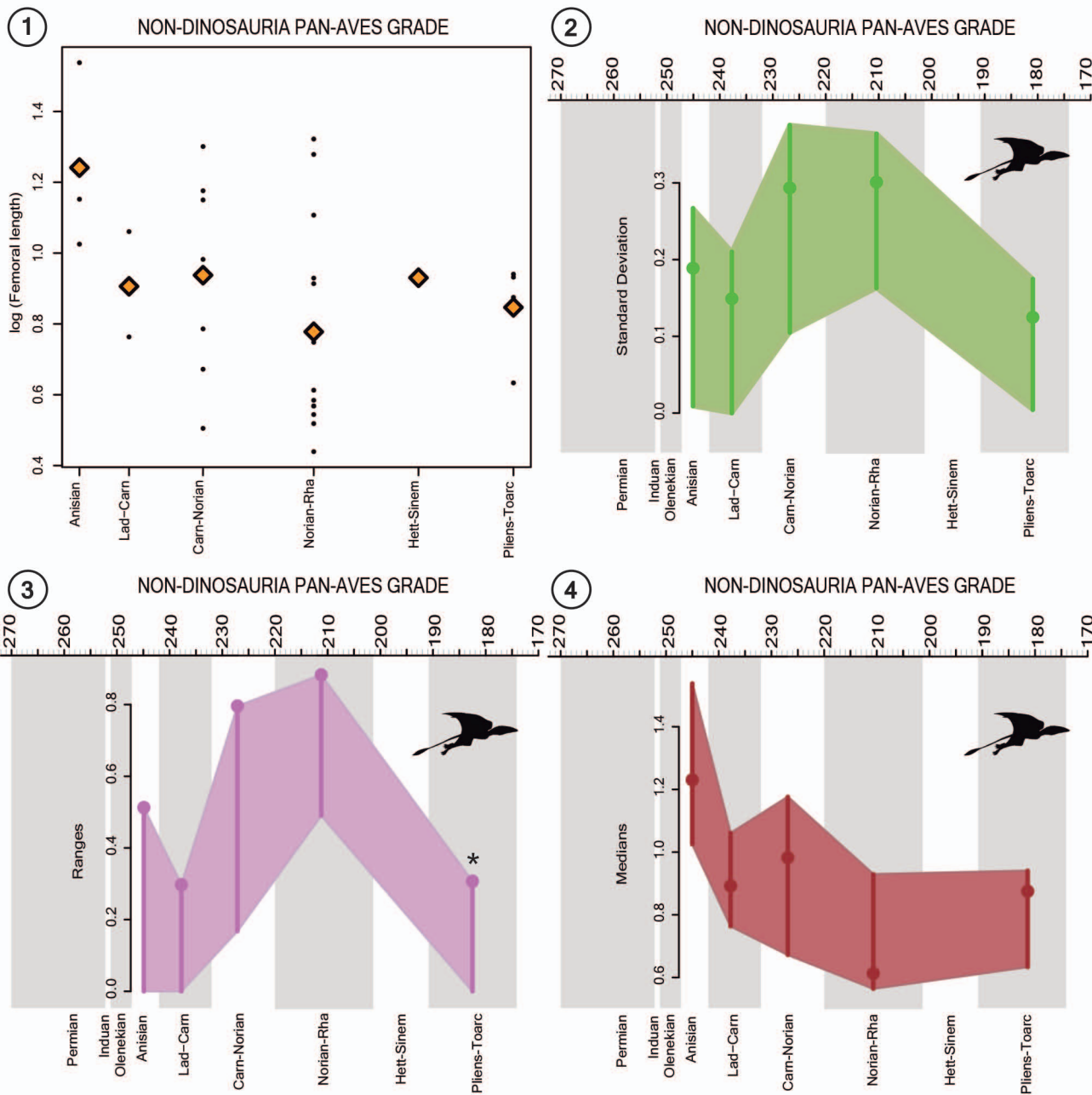


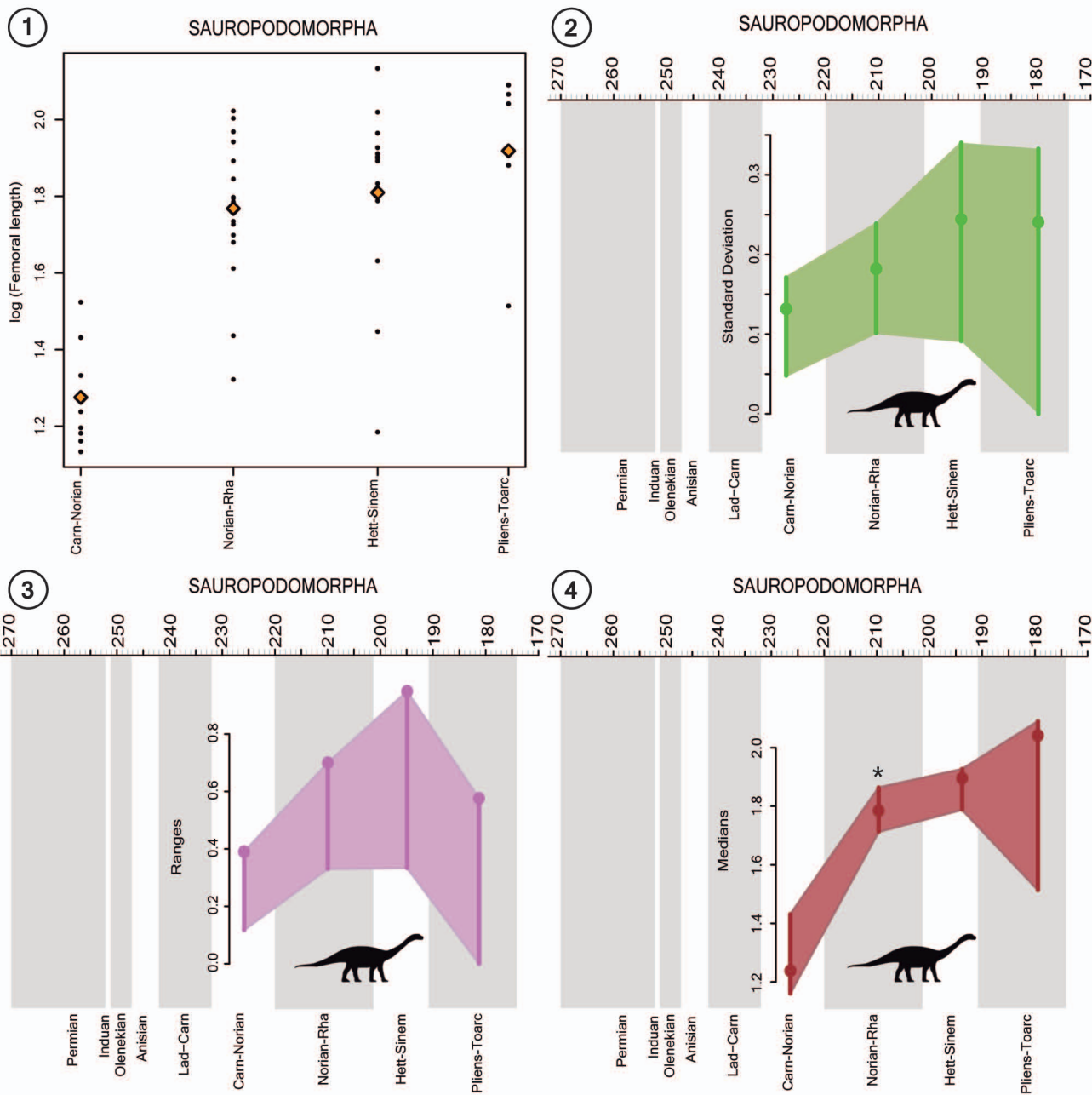


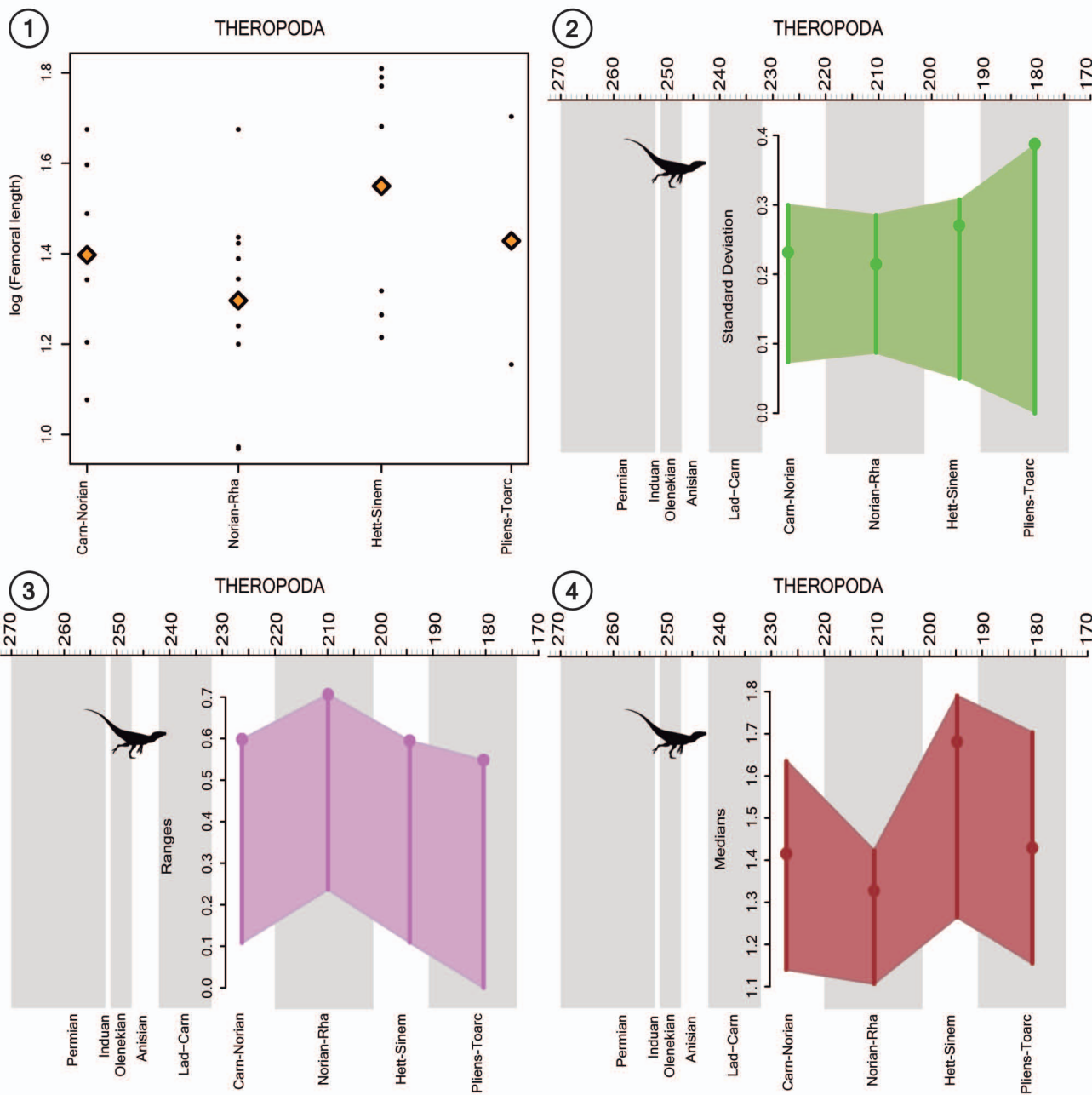


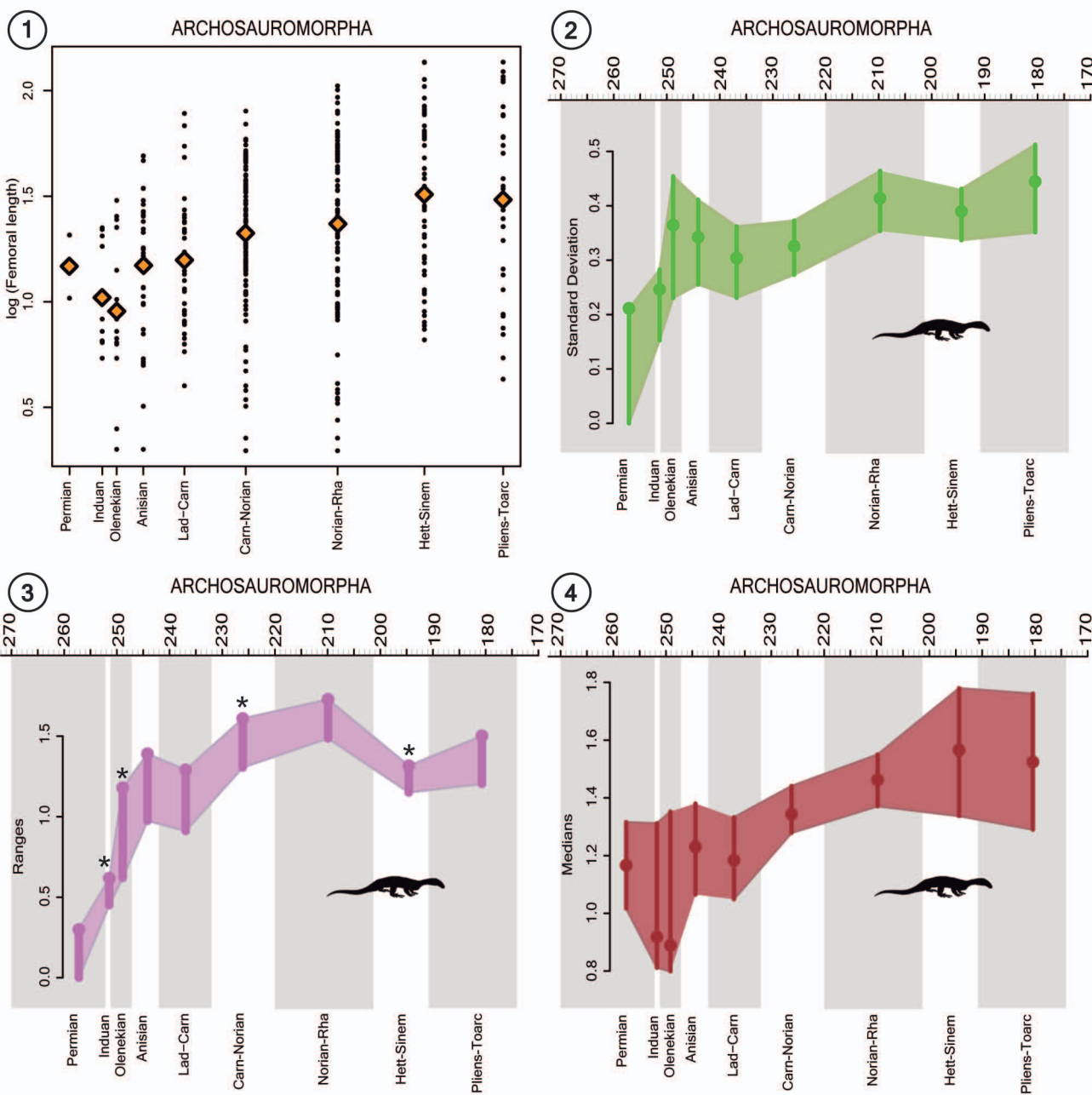


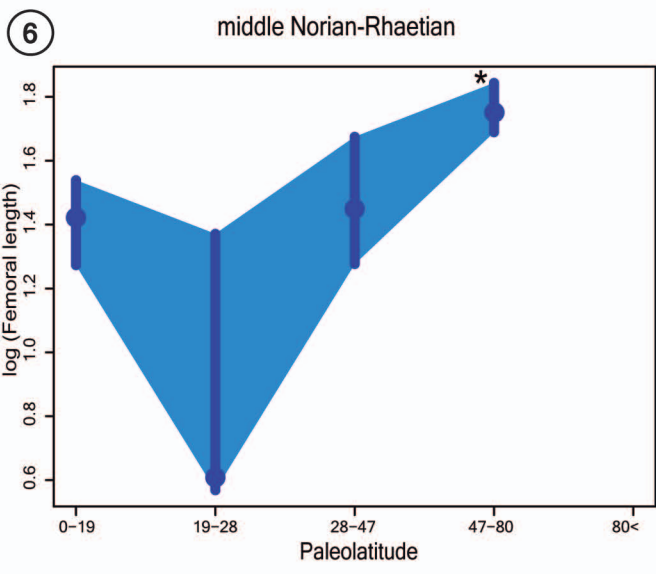
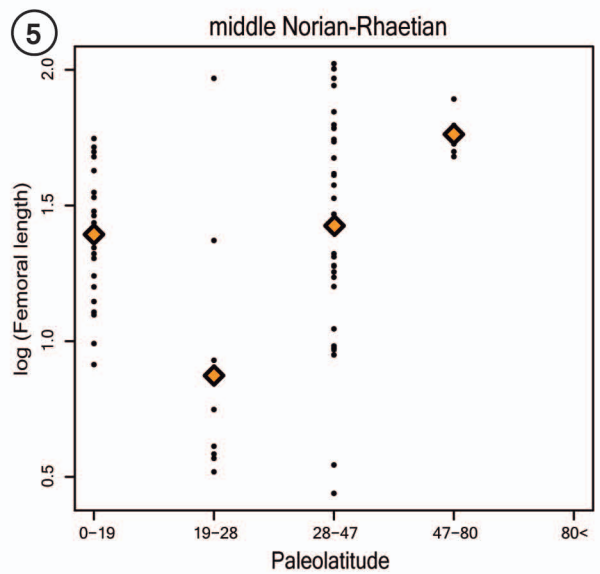
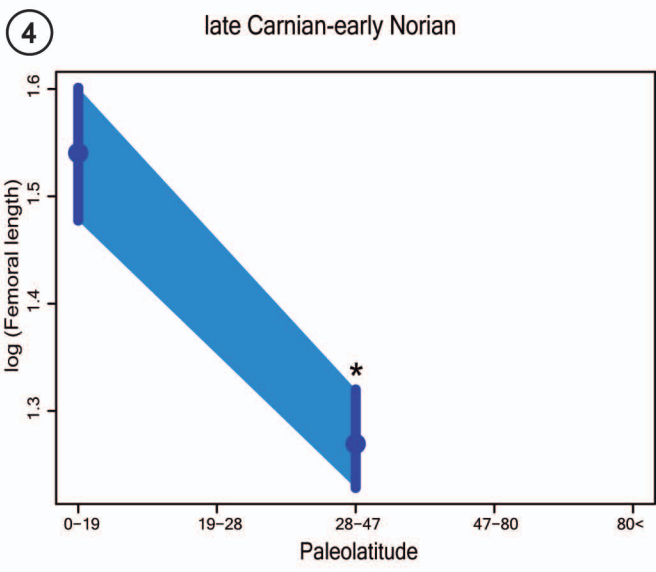
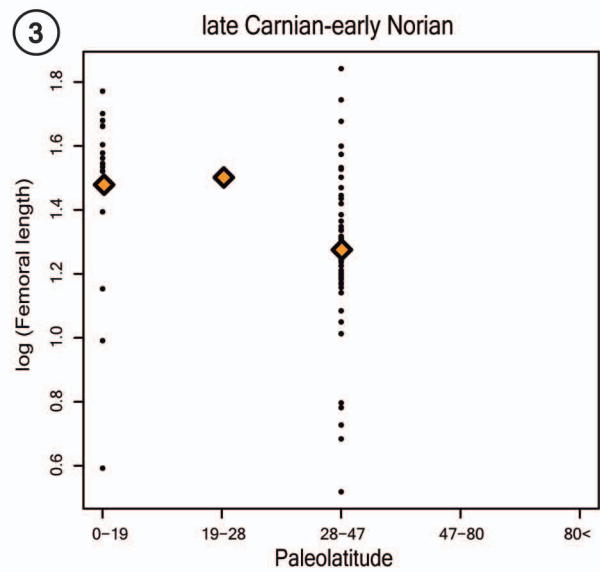
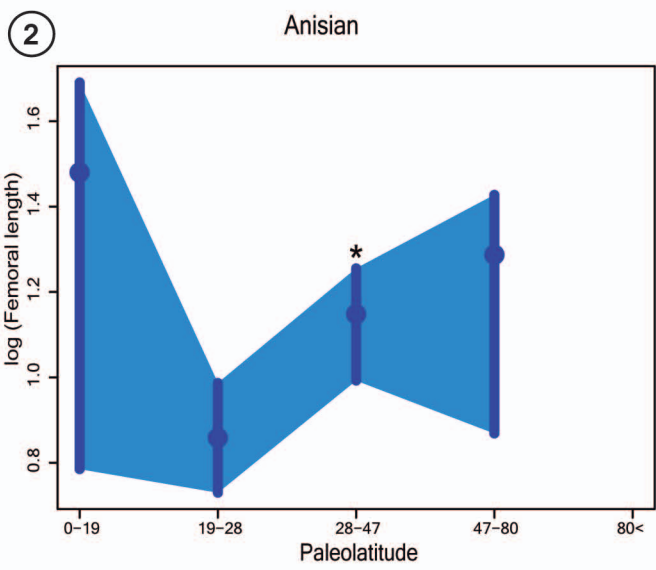
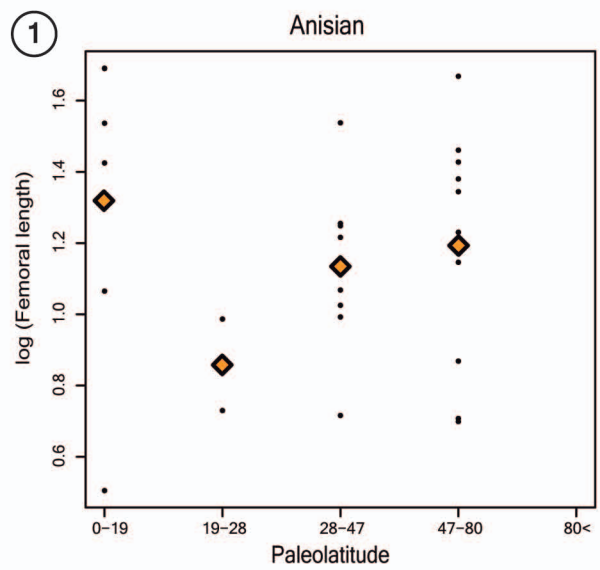


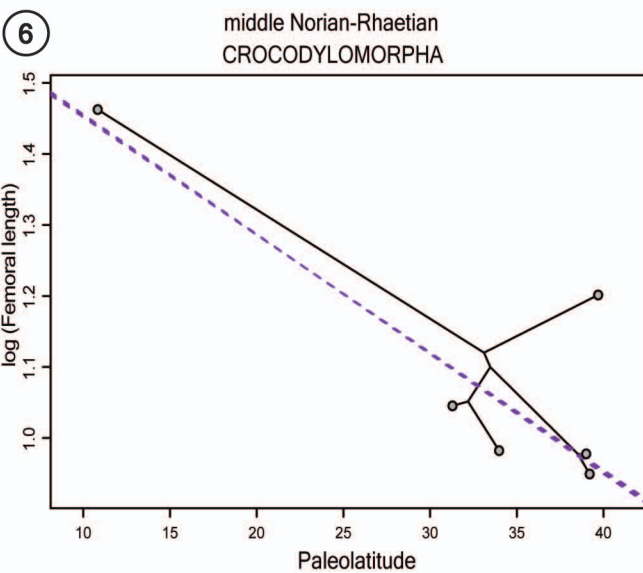
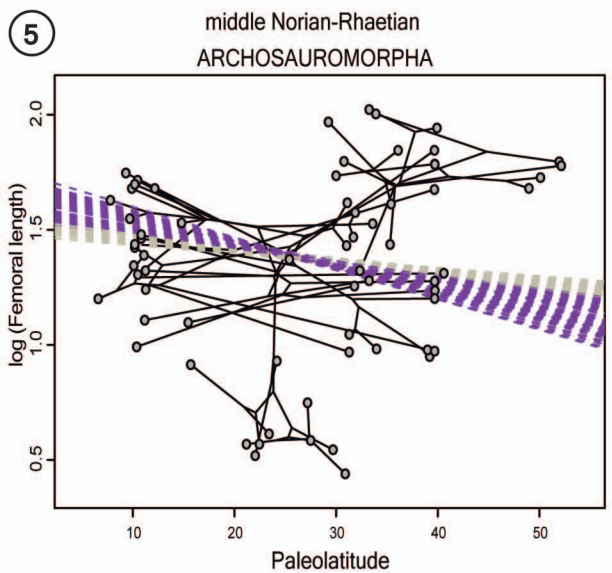
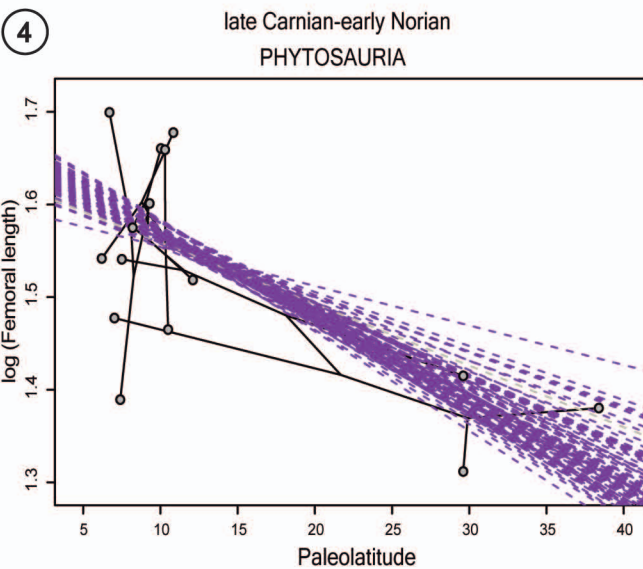
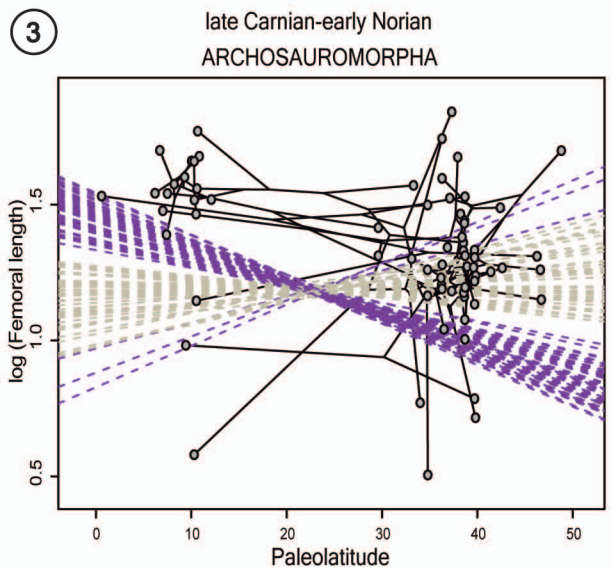
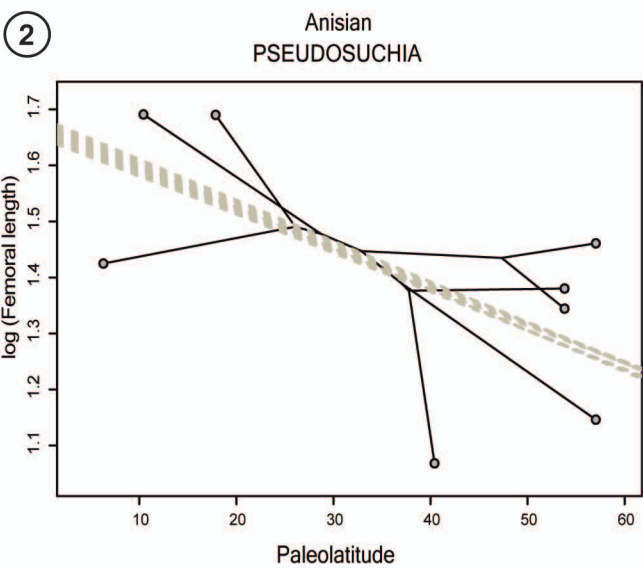
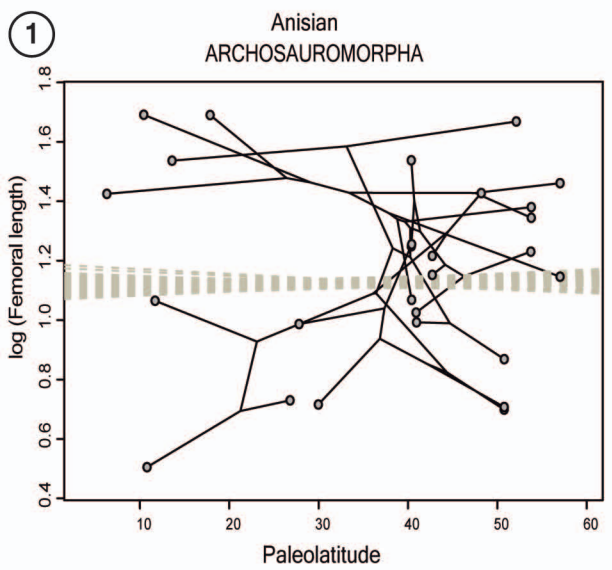








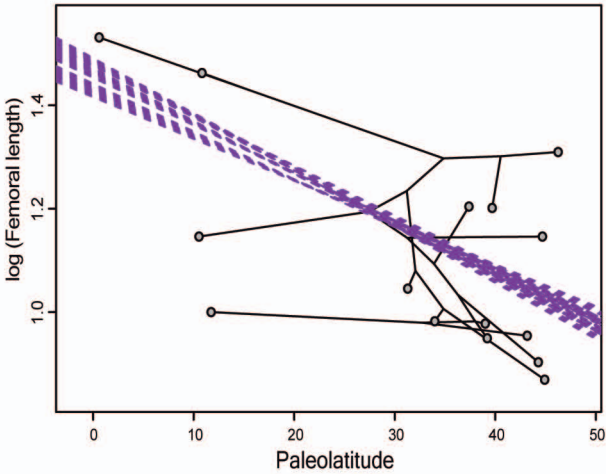




1

All Triassic

## CROCODYLOMOPRHA



2

All Triassic

## PHYTOSAURIA

